Gondwana Research xxx (2014) xxx–xxx

Contents lists available at ScienceDirect

Gondwana Research

journal homepage: www.elsevier.com/locate/gr

Geochemistry, Re–Os isotopes and highly siderophile element abundances in the Eastern Pontide peridotites (NE Turkey): Multiple episodes of melt extraction–depletion, melt–rock interaction and fertilization of the Rheic Ocean mantle

Abdurrahman Dokuz [a,*], İbrahim Uysal [b], Yildirim Dilek [c], Orhan Karsli [d], Thomas Meisel [e], Raif Kandemir [d]

[a] Department of Geol. Engineering, Gümüşhane University, Bağlarbaşı, 29000 Gümüşhane, Turkey
[b] Department of Geological Engineering, Karadeniz Technical University, 61080 Trabzon, Turkey
[c] Department of Geology & Env. Earth Science, Miami University, Oxford, OH 45056, USA
[d] Department of Geological Engineering, Recep Tayyip Erdoğan University, Rize, Turkey
[e] Department of General and Analytical Chemistry, University of Leoben, Franz-Josef-Str. 18, A-8700 Leoben, Austria

ARTICLE INFO

Article history:
Received 22 February 2013
Received in revised form 21 December 2013
Accepted 22 December 2013
Available online xxxx

Keywords:
Highly siderophile elements
Re–Os isotopes
Melt extraction
Melt–rock interaction and peridotite refertilization
Eastern Pontide belt (NE Turkey)

ABSTRACT

We report on the structure, geochemistry, Re–Os isotopes and relative abundances of highly siderophile elements (HSEs) of the Paleozoic peridotite–basalt occurrences in the Eastern Pontide belt of northeastern Turkey. These peridotites and the associated basaltic rocks are the remnants of the Rheic oceanic lithosphere, incorporated into the Eurasian continental margin during the Variscan (Hercynian) orogeny. The peridotites display a complex record of multiple magmatic, metasomatic and metamorphic events in different tectonic settings during the evolution of the Rheic upper mantle. The Beyçam harzburgite (BH) contains low Al_2O_3 (0.51–1.88 anhydrous wt.%) and high MgO (41.35–42.34 wt.%) contents, and its bulk-rock trace element compositions are less than 10% of the primitive upper mantle (PUM) values. The platinum, Pd and Re contents of the Beyçam harzburgite are highly depleted, whereas its Os, Ir, and Ru contents are slightly enriched relative to the PUM values. Its Pd and Re contents that are higher than those of the fertile Pulur lherzolite (PL) to the south and the absence of an isochronous relationship between its $^{187}Os/^{188}Os$ and $^{187}Re/^{188}Os$ show that the trace element distribution and the isotope ratios of the Beyçam harzburgite were significantly modified after the first melt-extraction episode. The first melt extraction occurred beneath the Rheic mid-ocean ridge spreading center, whereas the second melt extraction occurred in a mantle wedge above a Rheic subduction zone. The primary magmatic phases of the Pulur lherzolite show the geochemical characteristics typical for fertile lherzolite, formed in the early stages of oceanic lithosphere generation subsequent to the continental break up. The Pulur lherzolite also contains a secondary magmatic phase in the form of networks of clinopyroxene veins and channels, which are interpreted as an evidence for solid state melt–rock reactions between the lherzolite and a percolating basaltic melt above a subduction zone. This clinopyroxene addition resulted in the formation of variable concentrations of Al_2O_3 (2.47–4.33 wt.%) and MgO (29.76–40.10 wt.%) in the lherzolite. The rhenium, Pd and Pt concentrations of the Pulur lherzolite are depleted relative to the PUM values, whereas the Os, Ir and Ru concentrations are in the range of the PUM values as commonly observed in peridotites with a melt depletion history. The high suprachondritic $^{187}Os/^{188}Os$ is, however, inconsistent with a simple melt depletion history, and can be explained by the addition of radiogenic Os-bearing sulfide phases into the lherzolite as a result of melt–rock reactions. Basaltic rocks with an island arc tholeiitic composition from the Beyçam area represent the partial melting product of the moderately depleted Beyçam harzburgite and the basaltic parental melt from which the clinopyroxene precipitated. The covariation between the $^{187}Re/^{188}Os$ and $^{187}Os/^{188}Os$ of these basaltic rocks defines an isochron age of 377 ± 8 Ma (late Devonian). The combined structural, geochemical and isotope data indicate a prolonged history of multiple episodes of melt extraction–depletion, and melt–rock interaction and fertilization of the mantle lithosphere of the Rheic Ocean.

1. Introduction

Peridotitic rocks in ophiolites provide us with the best opportunities to observe in three-dimensions the structural, mineralogical and compositional variations in the upper mantle of ancient oceanic lithosphere (Boudier and Coleman, 1981; Dilek and Delaloye, 1992; Dilek and Eddy, 1992; Varfalvy et al., 1996; Zhou et al., 1996; Dilek and Flower, 2003; Piccardo, 2003; Dijkstra et al., 2004; O'Driscoll et al., 2012). However, the primary structures, whole-rock chemistry, and mineralogical compositions of these rocks may have been modified or obliterated by various processes, including interaction with

* Corresponding author. Tel.: +90 456 233 74 25; fax: +90 456 233 74 27.
E-mail address: dokuzabdurrahman@gmail.com (A. Dokuz).

1342-937X/$ – see front matter © 2013 International Association for Gondwana Research. Published by Elsevier B.V. All rights reserved.
http://dx.doi.org/10.1016/j.gr.2013.12.010

asthenospheric melts, mixing with recycled oceanic crust and sediments in the deep mantle, reaction with slab-derived fluids or melts in the mantle wedge, and extensional exhumation (Dilek and Rowland, 1993; Edwards and Malpas, 1996; Bodinier and Godard, 2003; Dilek and Robinson, 2003; Donnelly et al., 2004; Anderson, 2006; Ishikawa et al., 2007; Yoshikawa and Ozawa, 2007; Dilek and Furnes, 2009; Dilek and Thy, 2009; Stracke and Bourdon, 2009; Wong et al., 2010; Bézard et al., 2011; Dilek and Furnes, 2011; González-Jiménez et al., 2011; Xu et al., 2011; Brandl et al., 2012; Rajabzadeh et al., 2013). Systematic covariations of major and trace element distributions and modal variations reported from upper mantle rocks have been explained mainly by partial melting and melt extraction processes (Frey et al., 1985; Bodinier, 1988; Bodinier and Godard, 2003; Walter, 2003). However, some recent studies have shown that variable degrees of refertilization of a refractory protolith may produce similar modal compositions and chemical trends (Saal et al., 2001; Flower and Dilek, 2003; Müntener et al., 2004; Beyer et al., 2006; Le Roux et al., 2007; Rampone and Borghini, 2008; van Acken et al., 2008; Dilek and Morishita, 2009; Harvey et al., 2010; Uysal et al., 2012), and that most peridotites were refertilized after an earlier period of melt depletion (Elthon, 1992; Takazawa et al., 2000; Müntener et al., 2004; Brunelli et al., 2006; Batanova et al., 2008; van Acken et al., 2008; Dilek and Furnes, 2011). Addition of secondary clinopyroxene from percolating basaltic melts during porous melt flow and melt–rock reaction seems to have been a common process during the evolution of some abyssal peridotites (Seyler et al., 2007) and orogenic ultramafic massifs, such as Horoman from Japan (Saal et al., 2001; Toramaru et al., 2001), Erro–Tobbio from the Ligurian Alps (Rampone et al., 2004), Lherz from France (Le Roux et al., 2007), Totalp from the Swiss Alps (van Acken et al., 2008), and Mt. Maggiore from Corsica (Rampone et al., 2008). All these peridotites demonstrate structural and mineralogical evidence for peridotite–pyroxenite mixing at various scales during such refertilization events.

Some of the most effective geochemical tools for determining the mode and nature of upper mantle processes, including refertilization as recorded in ophiolitic peridotites, is to measure the absolute and relative abundances of highly siderophilic elements (HSE; including Re, Os, Ir, Ru, Rh, Pt, and Pd) and $^{187}Os/^{188}Os$ in the bulk upper mantle (e.g., Snow and Reisberg, 1995; Rehkämper et al., 1999a, 1999b; Morgan et al., 2001; Shi et al., 2007; Walker, 2009; Aldanmaz et al., 2012; Shi et al., 2012).

Os displays highly compatible behavior, whereas Re moderately incompatible during partial fusion of the upper mantle (Morgan, 1986; Hauri and Hart, 1997; Shirey and Walker, 1998; Burton et al., 2000). $^{187}Os/^{188}Os$ ratios of the residual peridotites evolve to subchondritic values due to re-depletion during partial melting. Conversely, partial melts with a large Re/Os develop highly suprachondritic $^{187}Os/^{188}Os$ values (e.g., Schiano et al., 1997; Roy-Barman et al., 1998; Shirey and Walker, 1998). However, following the melt depletion, smaller-scale processes, including melt percolation and crustal recycling, commonly perturb the HSE systematics of the upper mantle peridotites (e.g., Pearson et al., 1995; Brandon et al., 1996; Lorand et al., 1999; Becker et al., 2001; Lorand et al., 2004; Reisberg et al., 2005; Becker et al., 2006).

Melt percolation through porous flow at high melt/rock ratios may result in the formation of replacive dunites and harzburgites (Kelemen et al., 1995). Removal of pyroxenes during this open-system process may then cause lower than normal abundances of the compatible Ir group PGE (Os, Ir, Ru), low-Re abundances, and commonly chondritic to suprachondritic $^{187}Os/^{188}Os$ in the modified peridotites (Becker et al., 2001; van Acken et al., 2008). These variations have been reported from spatially constrained Re–Os studies of some peridotite massifs, indicating that the dissolution of pyroxenes and sulfides in a percolating basic melt and addition of radiogenic Os from such melts are common processes (Büchl et al., 2002, 2004). Similar compositional features have also been reported, albeit less abundantly, from peridotite xenoliths (e.g., Brandon et al., 1999; Handler et al., 1999; Schmidt and Snow, 2002; Pearson et al., 2003, 2004; Handler et al., 2005; Reisberg et al., 2005) and from abyssal peridotites (Standish et al., 2002; Harvey et al., 2006). However, melt percolation at a low melt/rock ratio causes the addition of basaltic components to the previously depleted peridotite, as the percolating melt may precipitate pyroxenes and sulfides (refertilization) (Bodinier and Godard, 2003; Pearson et al., 2003).

In this paper we present geochemical, highly siderophilic element (HSE) abundance and Re–Os isotope data from two peridotite massifs (Beyçam and Pulur) and associated basaltic rocks in the Eastern Pontide belt of NE Turkey (Fig. 1). We show that these mafic–ultramafic rocks, which represent the remnants of the Rheic oceanic mantle lithosphere had a complex history, including multiple episodes of partial melting, melt extraction–depletion, metasomatism–refertilization, and melt–rock interactions in different tectonic settings at various stages of their evolution. These findings suggest that this kind of multi-stage evolution of upper mantle peridotites via variable degrees of melting–metasomatism–refertilization processes is likely to be more common, particularly in SSZ ophiolites, than previously thought.

2. Geology of the pre-Jurassic basement rocks in the Eastern Pontides

The Pontides block in northern Turkey includes three major tectonic zones, Strandja, Istanbul and Sakarya (Okay et al., 2006). The latter, also known as the Sakarya continent, has early to middle Carboniferous high-T/low to medium-P metamorphic basement with syn- to post-collisional granitoid intrusions (Yilmaz et al., 1997; Okay et al., 2006; Eyuboglu et al., 2011; Sarifakioglu et al., 2013). These rock units of the Sakarya continent collectively represent the artifacts of a protracted collisional orogeny (Variscan or Hercynian orogeny) that developed in the late Paleozoic (Dilek, 2006; Okay et al., 2006; Nance et al., 2010; Murphy et al., 2011).

Recent studies (Topuz et al., 2004, 2007; Eyuboglu et al., 2010; Dokuz, 2011; Dokuz et al., 2011) have shown that the Paleozoic rock assemblages of the Sakarya continent in the Eastern Pontides make up four main tectonic units: (1) low- to medium-grade subduction–accretion complex; (2) early to middle Carboniferous, high-T/low-P continental metamorphic rocks composed of gneiss, schist, migmatite, amphibolite and marble; (3) middle to late Carboniferous syn- to post-collisional granitoid plutons; and (4) Permo-Carboniferous sedimentary rocks of a molasse origin.

Serpentinized mafic to ultramafic rocks and phyllites within the Kurtoğlu, Beyçam and Pulur metamorphic complexes (Fig. 1a) represent a subduction–accretion complex of the Rheic Ocean (Dokuz et al., 2011). In the Pulur area, a low-grade tectonic unit, including basaltic rocks with MORB affinities, peridotite blocks, and a phyllitic sequence consisting of calcareous phyllite, marble, quartzo-feldspathic schist and meta-chert is exposed in tectonic windows within an early Carboniferous high-temperature tectonic unit (Topuz et al., 2004, 2007; Fig. 1b). Peridotite blocks in the Pulur area consist of moderately serpentinized lherzolite, whereas in the Beyçam area they are made of strongly serpentinized harzburgite (Fig. 1c). The Pulur lherzolite displays the typical geochemical and mineralogical features of fertile orogenic lherzolites (Dokuz et al., 2011), which are widely interpreted as an early stage oceanic lithosphere formation following the continental break up and rifting.

Mineralogical and geochemical features of the Beyçam harzburgite resemble those of the moderately depleted residues formed in a mantle wedge in a suprasubduction zone (SSZ) setting (Dokuz et al., 2011). These upper mantle peridotites were emplaced northward onto the southern margin of the Sakarya continent in the early Carboniferous (Dokuz et al., 2011). The terminal closure of the Rheic oceanic tract was followed by the collision of a peri-Gondwana terrane with the Sakarya continent and by the imbrication of its continental margin rocks along north-directed thrust faults on top of the remnants of the Rheic oceanic

Please cite this article as: Dokuz, A., et al., Geochemistry, Re–Os isotopes and highly siderophile element abundances in the Eastern Pontide peridotites (NE Turkey): Multiple episodes ..., Gondwana Research (2014), http://dx.doi.org/10.1016/j.gr.2013.12.010

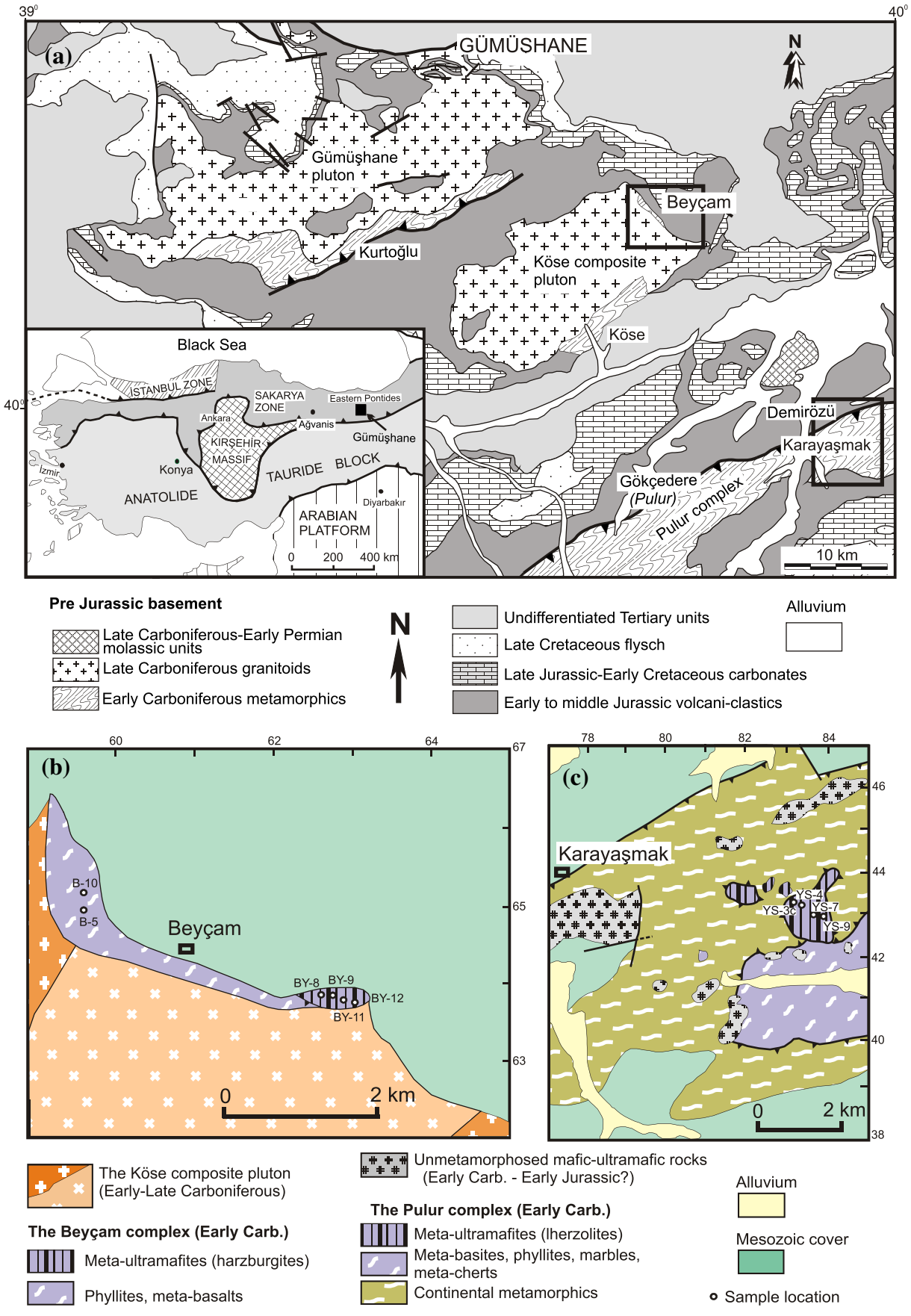

Fig. 1. a. Geological map of the Gümüşhane region in the Eastern Pontide belt of NE Turkey, showing the distribution of the Variscan basement and the Mesozoic–Cenozoic cover units. Inset shows the main tectonic units of Turkey (modified from Okay et al., 2006). b and c. Detailed geological maps of the Beyçam and Pulur areas, respectively, showing the distribution of orogenic peridotites within the Variscan basement and the sample locations. Modified from Dokuz et al. (2011)

Please cite this article as: Dokuz, A., et al., Geochemistry, Re–Os isotopes and highly siderophile element abundances in the Eastern Pontide peridotites (NE Turkey): Multiple episodes ..., Gondwana Research (2014), http://dx.doi.org/10.1016/j.gr.2013.12.010

lithosphere (Beyçam and Pulur peridotites) and the Sakarya continental crust. This tectonic burial of the remnants of the Rheic oceanic lithosphere resulted in their metamorphism under lower amphibolite facies conditions. The syn- to post-collisional granitoid plutons (i.e. Gümüshane and Köse plutons) were emplaced into the Variscan orogenic crust during 322–304 Ma (Dokuz, 2011; Kaygusuz et al., 2012). The ensuing tectonic uplift and erosion caused the exhumation of the crystalline basement rocks and accumulation of late Kasimovian molasse-type deposits in a terrestrial or shallow marine basin (Okay and Leven, 1996; Kandemir and Lerosey-Aubril, 2011). The exhumed Variscan orogenic crust was unconformably overlain by the Jurassic clastic sedimentary rocks (Dokuz and Tanyolu, 2006; Şen, 2007; Kandemir and Yılmaz, 2009; Dokuz et al., 2010; Ustaömer and Robertson, 2010).

3. Analytical methods

In this study, we analyzed eight samples of the representative peridotites (Pulur lherzolite and Beyçam harzburgite) and two samples of the representative basaltic rocks for Re–Os isotopes and HSE abundances, and for major, trace and rare earth elements (previously reported in Dokuz et al., 2011). We also utilized a larger geochemical database (major, trace and rare earth element chemistry) from these peridotites based on our previous investigations in this area. The samples of this study were crushed in steel crushers and ground in an agate mill to a grain size of <200 mesh. Major element analyses of the samples were determined at the ACME Laboratories Ltd. in Vancouver, Canada, using ICP-AES after fusion with $LiBO_2$ with detection limits of approximately 0.001–0.04%. The sample preparation and analytical methods are explained in Appendix I.

Concentrations of the rare earth elements (REEs) and some trace elements (Rb, Sr, Y, Zr, Cs, Ba, Hf, Nb, Ta, U, and Th) of all the samples were determined by inductively coupled plasma-mass spectroscopy (ICP-MS, Thermo Scientific X Series II) in the Department of Earth Sciences at University of Durham. We followed a standard nitric and hydrofluoric acid digestion technique for these analyses (Ottley et al., 2003). Due to the low concentration of many of the elements of interest, special care was required to minimize sample contamination. Sample preparation was undertaken in clean-air laminar flow hoods.

The samples were analyzed for HSE (Os, Ir, Ru, Pt, Pd, Re) concentrations and $^{187}Os/^{188}Os$ isotope ratios, using the isotope dilution technique described by Meisel et al. (2003) and Paliulionyte et al. (2006) and utilizing a quadrupole ICP-MS system (HP 7500, Agilent Technologies) at the Montanuniversitaet Leoben, Austria. The analytical techniques are explained in Appendix II.

4. Petrography

The Beyçam peridotite consists of moderately to strongly serpentinized harzburgites, which show an anastomosing foliation identified by long, continuous, wavy cleavage domains occupied predominantly by Fe-hydroxide, magnetite and spinel that formed an irregular network outlining lenticular microlithons of serpentine minerals (Fig. 2a). The Pulur peridotite is composed of slightly to moderately serpentinized spinel lherzolites, which locally contain irregular, mm- to a few cm-wide hornblendite veins (Fig. 2b). Olivine, orthopyroxene and spinel are the primary igneous phases that are partly preserved following the subsequent serpentinization and metamorphic processes (Dokuz et al., 2011). Clinopyroxene could not be observed in any of the spinel lherzolite samples, but amphibole with a magnesio-hornblende composition [Mg-number ($Mg/(Mg + Fe^{2+})$) = 87–91; Supplementary Table] is widespread in them showing a well-preferred orientation (Fig. 3a). Some other amphibole grains display a cumulate texture with a weak orientation (Fig. 3b), particularly along the irregular veins crosscutting the serpentine minerals and the primary igneous phases. Magnesio-hornblende (pseudomorph after clinopyroxene) in the veins can be differentiated from the original hornblende based on its relatively low Mg-number (61–67; Fig. 4).

Tremolite in the lherzolitic rocks is a product of retrograde metamorphic reactions, developed during the Variscan orogeny, and forms tabular crystals exhibiting well-defined cleavage planes and including poikilitic serpentine minerals (Fig. 3c). Locally, it occurs as a pseudomorph after orthopyroxene (Fig. 3d). Some tremolite grains are entirely or partially transformed into small aggregates of tremolite along their margins. Serpentine is an alteration product after olivine and orthopyroxene.

We sub-group the amphiboles in the Pulur lherzolite into four types based on our petrographic observations (Fig. 3) and microprobe analyses (Fig. 4). The first type shows homogeneous distribution and a preferred orientation (Fig. 3a) in most of the samples. We interpret this amphibole as metamorphic hornblende, which replaced the magmatic clinopyroxene during the Variscan orogeny. The second type with a similar composition is distinguished from the first type by its cumulate-like appearance along mm- to cm-long, sub-parallel irregular veins or conduits (Fig. 2b). These amphibole grains also show a well-defined foliation. The third type amphibole differs from the other two types by its weakly oriented cumulate texture and significantly lower Mg-number. In addition to these three types of amphiboles, tremolite is the fourth type of amphibole in the Pulur lherzolite. Tremolite has been found either as a pseudomorph after orthopyroxene (Fig. 3c, d) or as stellar crystals in irregularly distributed fissures in the lherzolite,

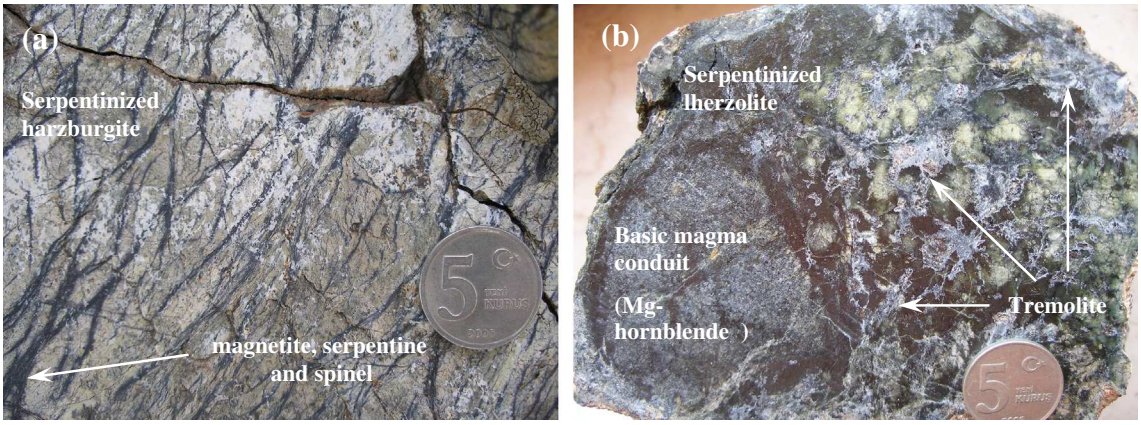

Fig. 2. a. Anastomosing foliations of magnetite, serpentine and spinel crystals outlining lenticular serpentine microlithons in a hand specimen of the harzburgite from the Beyçam area. b. Photograph of a hand specimen showing a conduit filled with hornblende that was retrograded after clinopyroxene and tremolite after orthopyroxene in the fertile Pulur lherzolite. The coins are 1.7 cm in diameter.

Please cite this article as: Dokuz, A., et al., Geochemistry, Re–Os isotopes and highly siderophile element abundances in the Eastern Pontide peridotites (NE Turkey): Multiple episodes ..., Gondwana Research (2014), http://dx.doi.org/10.1016/j.gr.2013.12.010

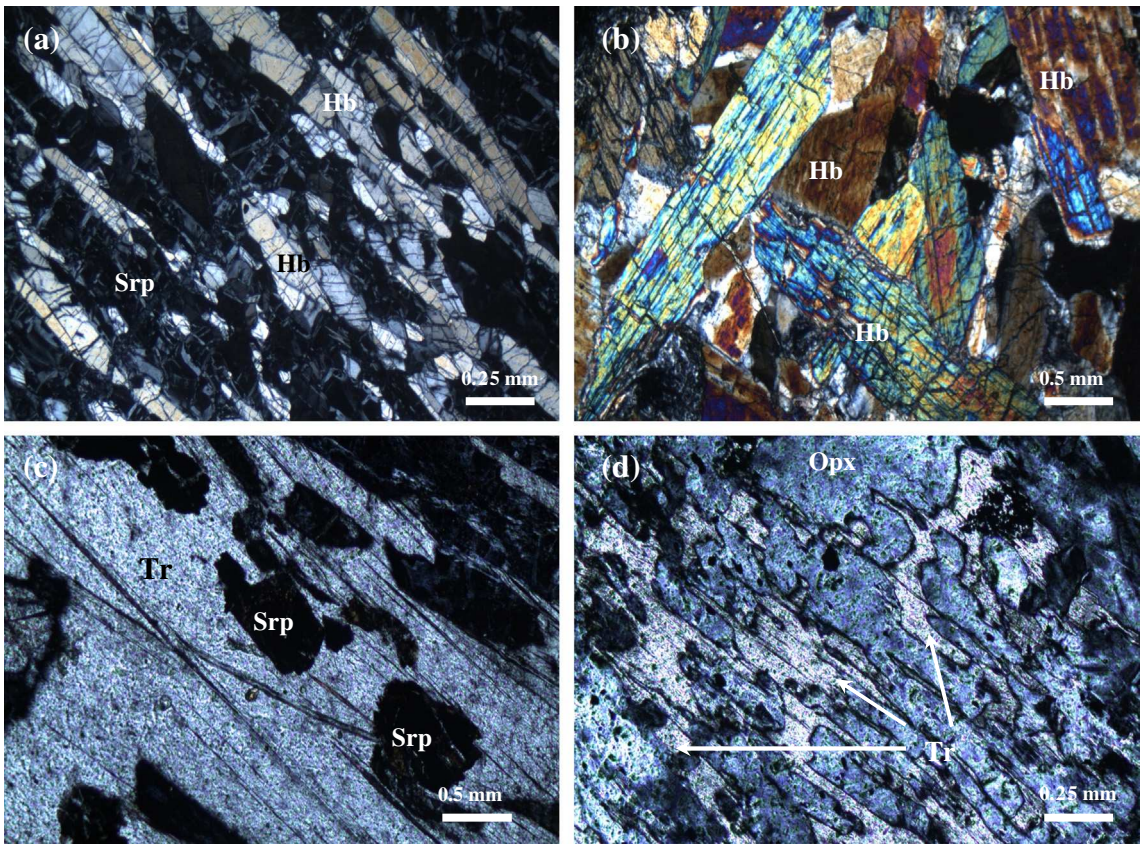

Fig. 3. Microtextures in the Pulur lherzolite samples. a. Homogenous distribution and well-preferred orientation of hornblende (after primary clinopyroxene) in the lherzolite. b. Cumulus hornblende in a veinlet of Pulur lherzolite. The clinopyroxene precursor of this hornblende precipitated from an upward percolating basaltic melt. c. Megacryst of tremolite retrograded after earlier primary orthopyroxene, including poikilitic serpentine and earlier primary olivine. d. Primary orthopyroxene porphyroblast partly replaced by tremolite, which shows cleavages possessing the same orientation as those of the orthopyroxene. Srp: serpentine, Hb: hornblende, Tr: tremolite, Opx: orthopyroxene.

and it is a metamorphic mineral that formed during the Variscan metamorphism.

The basaltic rocks occur in 1- to 3-m-thick, lenticular domains subparallel to the foliation planes in the phyllites. The primary mineral phases include plagioclase, clinopyroxene, amphibole (ferro-tschermakite to ferro-hornblende, Fig. 4) and opaque minerals; the accessory phases are made of quartz, chlorite, and sericite. Thin (1-mm- to 2-cm-thick) quartzofeldspathic veins crosscut the foliation in the phyllites.

5. Alteration effects

5.1. Effects of serpentinization

The degree of serpentinization is high in the harzburgite and lherzolite samples with LOI contents of 10.1 to 14.6 wt.%, except for sample YS-3C (Table 1). Such a high, low temperature volume change requires that the mobility of elements such as PGE and Re, and Os isotope composition during serpentinization processes must be considered before assessing their behavior at magmatic temperatures.

Serpentine minerals form principally after retrograde hydrothermal alteration of silicate minerals, particularly the olivine, or by prograde metamorphism after pre-existing serpentinite. As serpentinization is simply restricted to the addition of water or hydration of olivine and pyroxenes, it can largely be interpreted as an isochemical process (Paulick et al., 2006). However, a 10% increase in volume of H_2O in a peridotite rock would result in a 10% reduction in absolute abundances of elements compared to their unaltered precursors, even if the elements are perfectly immobile. Similar to the serpentinization, there is an increase in volume during the metamorphic transformation of diopside and augite to tremolite and hornblende. Volume change via addition of H_2O during these metamorphic transformations is restricted to 2 to 3% as observed in the microprobe analyses of the magnesio-hornblende and tremolite (Supplementary Table), implying negligible influence on the HSE concentrations and Os isotope composition of the lherzolite. Normalization of concentrations to volatile free basis can thus provide a reasonable approach for volatile free abundances of major elements, but the key question here is whether the same approach is valid for the Os and HSE isotope compositions of the rocks used in this study.

Osmium, Ir and Ru are only slightly affected by serpentinization because they are more abundant in olivine compared to Pt, Pd and Re. The lack of Re-compatible silicate minerals such as clinopyroxene and amphibole in the Beyçam harzburgite suggests that serpentinization almost has no effect on the absolute abundance of Pt, Pd and Re. In the Pulur lherzolite, transformation of clinopyroxenes to the magnesio-hornblende and tremolite rather than serpentine minerals is a common phenomenon, indicating that volume change by addition of H_2O is much more limited, and that the abundances of Re and, in part, Pt and Pd were not much affected. Furthermore, all these retrograde and prograde transformations have no effect on the modal volume of base metal sulfides controlling almost the entire abundance of the HSE of the residual peridotites.

Olivine, orthopyroxene, clinopyroxene and spinel are the major mineral phases in refractory peridotites that account for less than 30% of the whole-rock HSE budget (Luguet et al., 2007).

Of these, spinel and olivine, which dominate the harzburgitic residue, show the highest HSE concentration especially for Os, Ir and Ru, whereas the pyroxenes, which are predominant in lherzolitic peridotites are 1 to 2 orders of magnitude poorer (Righter et al., 2004;

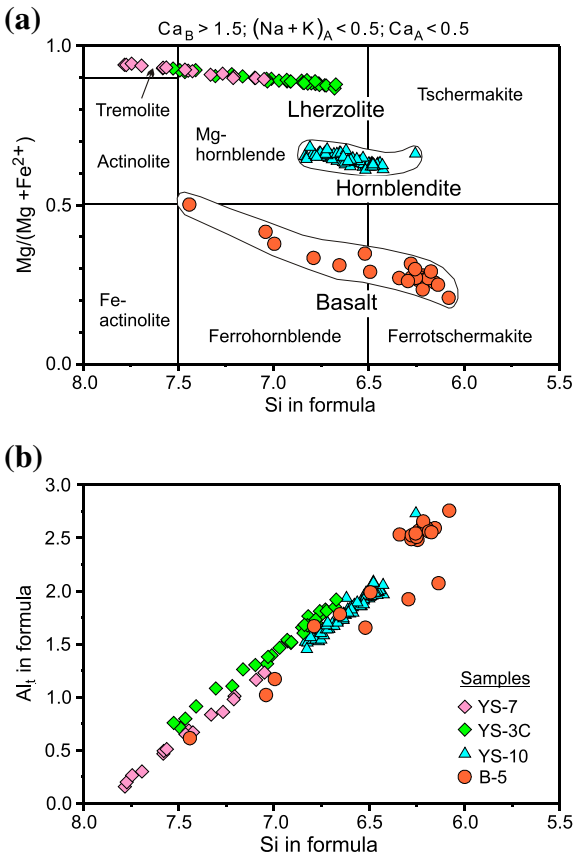

Fig. 4. a. Classification of the calcic amphiboles from the Pulur lherzolite, hornblendite dike (Pulur area) and basaltic rock (Beyçam area). b. Si vs. Al variation diagram of the amphiboles.

Brenan et al., 2005). Considerable enrichment of Re relative to Pt and Pd in basalt, as evidenced in this study, shows that Re, as the most lithophile element among the HSE, may behave more incompatible than Pt and Pd during partial melting, and that it gets incorporated into silicate minerals (e.g. clinopyroxene and amphibole), found in basalt (Righter and Hauri, 1998; Righter et al., 2004; Mallmann and O'Neill, 2007). On the other hand, Ru–Os ± Ir sulfides and Pt–Ir ± Os alloys, which are micron- to submicron-sized platinum group minerals, account for 70–100% of the HSE budget in the refractory depleted harzburgite (Luguet et al., 2007). These observations suggest that silicate–sulfide partitioning of HSE for the silicate minerals of the mantle residues is negligible and that the HSE budgets of the mantle residues are almost entirely controlled by base metal sulfides.

Another likely effect of serpentinization on the element mobility is the addition of elements into mantle peridotites during their interaction with seawater. Fluid mobile elements such as Sr, Ba, U and Re in abyssal peridotites close to seafloor show elevated concentrations, which are interpreted to result from their interaction with seawater (Harvey et al., 2006). Seawater has Re concentration much higher than Os (Re/Os ≈ 740) (Anbar et al., 1992; Levasseur et al., 1998), whereas sulfide minerals, which have a low Re/Os ratios (Re/Os ≤ 1.0) (Burton et al., 1999; Alard et al., 2002), control the HSE budget in abyssal peridotites. However, some previous studies (Burnham et al., 1998; Rehkämper et al., 1999a, 1999b; Büchl et al., 2002; Harvey et al., 2006; van Acken et al., 2010) have found no correlation between the degree of serpentinization in the peridotites and their HSE concentrations and ratios.

The melt depletion indicator Al_2O_3 behaves in a rather immobile manner during the aqueous alteration processes (Snow and Dick, 1995; Staudigel et al., 1996). Consequently, the correlations of Al with the HSE and $^{187}Os/^{188}Os$ abundances and the ratios are commonly well preserved in serpentinized peridotites. Therefore, the linear correlations and deviations from the HSE of the melt extraction trends are primarily igneous in origin rather than due to serpentinization.

5.2. Effects of Variscan metamorphic overprint

The Rheic Ocean lithosphere emplaced onto the continental crust underwent deformation and metamorphism during the Variscan orogeny that resulted in the formation of a preferred alignment of magnetite and in the crystallization of magnesio-hornblende and tremolite in the serpentinized peridotites. Clinopyroxene (augite) in the lherzolite was replaced by magnesio-hornblende (Fig. 4). Tremolite includes poikilitic serpentine (Fig. 3c) and occurs as a pseudomorphic replacement of the orthopyroxene (Fig. 3d). Hornblende is stable under a wide range of pressure–temperature conditions from the upper greenschist through the amphibolite into the lower part of the granulite facies. However, the coexisting tremolite constrains the degree of metamorphism to upper greenschist facies because it normally converts to diopside at higher temperatures.

6. Results

6.1. Bulk-rock analyses

We present the representative whole-rock compositions of eight peridotite and two basaltic rock samples in Table 1, with a summary of the modal mineralogy calculated using a least squares linear regression. The high loss-on-ignition (LOI > 10 wt.%) values of the samples, except for YS-3C from the Pulur lherzolite, suggest that the analyzed rocks are serpentinized extensively. Therefore, in the following section, the volatile-free calculated major element data were used in order to reduce the effects of the variable dilution of the elements caused by serpentinization.

A distinctive feature of the Beyçam harzburgite is the reduced number of elemental abundances with a narrow range relative to those of the Pulur lherzolite. When the rock groups were evaluated comparatively, the whole-rock major element variations display a wide range from highly fertile compositions in the Pulur lherzolite (29.76–40.10 wt.% MgO and 2.47–4.33 wt.% Al_2O_3) to highly refractory compositions in the Beyçam harzburgite (e.g., 41.35–42.34 wt.% MgO and 0.51–1.88 wt.% Al_2O_3). Only sample YS-4 among the Pulur rocks demonstrates whole-rock geochemical and mineralogical compositions similar to those of the least-depleted Beyçam rocks.

A closer look at the lherzolite and harzburgite samples shows, however, different co-variation trends. On an Al_2O_3 vs. Cr diagram (Fig. 5), this difference between the harzburgite and lherzolite trends is evident. The harzburgite samples demonstrate curved positive correlations, whereas the lherzolite samples exhibit negative and even flat correlation in the most fertile rocks. Likewise, Fe_2O_3 and CaO display flat or slightly negative correlations for the harzburgite samples (not shown), whereas steep positive correlations are distinctive for the lherzolite samples.

The Beyçam harzburgite demonstrates mildly depleted rare earth element (REE) patterns that are characterized by an almost constant, slightly positive profile. Contrasting behaviors are shown by Zr and Hf; Zr shows negative troughs, whereas Hf commonly displays a positive anomaly. Niobium and Ta also demonstrate contrasting behaviors; compared to the Pulur samples, the magnitude of the positive Ta anomaly is increased in the Beyçam samples. The Pulur lherzolite samples display slightly enriched light REE and flat medium–heavy REE profiles similar to those of the undepleted abyssal peridotites (Bodinier and Godard, 2003). Compared with neighboring elements, Ti and Zr demonstrate distinctive negative spikes. In agreement with the clinopyroxene contents of the samples, we observe Sr enrichment relative to Pr and Nd. A distinctive positive spike is shown for Ta relative to Nb.

Please cite this article as: Dokuz, A., et al., Geochemistry, Re–Os isotopes and highly siderophile element abundances in the Eastern Pontide peridotites (NE Turkey): Multiple episodes ..., Gondwana Research (2014), http://dx.doi.org/10.1016/j.gr.2013.12.010

Table 1
Whole-rock major and trace element data for the Pulur and Beyçam peridotites and two basaltic rocks with the modal compositions of peridotites. (after Dokuz et al., 2011).

Sample	Beyçam Harzburgite				Pulur Lherzolite				Meta-basalt		DL	Blank (Average)	GP13 Average	GP13 StDev	GP13 RSD%
	BY-8	BY-9	BY-11	BY-12	YS-3C	YS-4	YS-7	YS-9	B-5	B-10					
Major oxides (%)												Stan.	Stan.	Stan.	
SiO_2	40.57	40.47	40.76	38.59	46.77	40.21	41.41	41.75	47.88	45.29					
TiO_2	0.01	0.01	0.02	0.01	0.18	0.04	0.07	0.12	1.58	1.66			0.100	0	2.64
Al_2O_3	1.17	0.84	1.65	0.43	4.10	2.16	2.95	3.16	22.05	21.75					
Fe_2O_3T	7.85	7.82	7.80	7.90	10.28	8.28	8.05	8.73	6.92	9.83					
MgO	36.04	36.59	35.86	35.90	28.15	35.12	32.82	32.28	2.89	3.86					
MnO	0.07	0.05	0.09	0.08	0.13	0.11	0.10	0.12	0.16	0.30			0.12	0	3.97
CaO	1.05	0.10	1.14	1.23	4.16	0.94	2.47	2.86	10.18	8.80					
Na_2O	0.01	0.01	0.02	0.06	0.27	0.05	0.07	0.09	2.18	1.17					
K_2O	<0.01	<0.01	0.01	<0.01	0.04	<0.01	0.01	<0.01	3.68	3.86					
P_2O_5	0.00	0.00	0.00	0.00	0.01	0.00	0.01	0.01	0.23	0.21					
Cr_2O_3	0.38	0.35	0.40	0.40	0.30	0.40	0.35	0.37	0.01	0.01					
LOI	12.20	12.90	11.40	14.60	4.90	11.80	10.90	10.10	1.90	2.90					
Sum	99.36	99.38	99.39	99.39	99.50	99.39	99.43	99.58	99.90	99.86					
Mg#	0.90	0.90	0.90	0.90	0.84	0.89	0.89	0.88	0.45	0.43					
Trace elements (ppm)															
Cr	2549	2473	2635	1920	2010	2616	2152	2052	43	41	0.2800	0.000	2193	72.00	3.13
Ni	2485	2540	2395	2367	1573	2190	1979	1716	32	30	0.3000	0.461	2164	202.0	9.31
Sc	8.0	6.9	9.7	5.8	18.0	10.9	14.9	16.4	21.0	21.1	0.1300	0.000	15.33	0.84	5.51
Co	107.0	108.4	105.4	97.2	81.4	100.5	98.6	88.2	20.6	31.7	0.0700	0.003	90.6	2.16	2.38
Ba	2.9	3.6	2.3	3.9	13.1	4.8	14.0	10.2	1202.0	1346.0	0.0026	0.002	0.58	0.01	2.31
Sr	2	1	3	6	155	23	51	95	1019	545	0.0050	0.004	10.10	0.16	1.63
Rb	0.3	0.2	0.7	0.1	1.1	0.3	0.2	0.7	122.5	160.7	0.0020	0.000	0.35	0.01	2.07
Cs	0.32	0.11	0.50	0.04	3.10	0.62	0.37	1.63	5.22	5.08	0.0024	0.000	0.07	0.00	3.33
Ga	1.0	0.7	1.2	0.4	4.6	2.3	2.4	3.3	21.1	23.3	0.0090	0.019	2.24	0.06	2.89
Th	0.00	0.00	0.00	0.00	0.14	0.05	0.17	0.13	1.03	1.07	0.0001	0.000	0.01	0.00	5.08
U	0.00	0.00	0.00	0.00	0.04	0.03	0.03	0.03	0.49	0.36	0.0001	0.000	0.00	0.00	13.98
Nb	0.0	0.0	0.0	0.0	2.4	0.9	1.2	1.7	14.6	16.5	0.0033	0.000	0.10	0.00	1.87
Ta	0.02	0.00	0.00	0.00	0.08	0.02	0.08	0.09	0.95	1.03	0.0001	0.004	0.01	0.00	0.00
Hf	0.05	0.00	0.01	0.00	0.17	0.03	0.11	1.35	2.00	1.62	0.0003	0.001	0.18	0.00	1.64
Zr	0.2	0.1	0.3	0.1	5.2	0.6	3.8	4.1	76.9	59.4	0.0130	0.012	5.80	0.03	0.47
Y	0.4	0.2	0.6	0.1	5.5	2.8	2.1	3.7	21.3	22.0	0.0005	0.000	3.55	0.04	1.00
V	29	21	40	14	125	46	48	67	172	243	0.0300	0.000	67.41	1.50	2.23
Pb	0.83	0.87	0.79	0.89	0.71	0.45	0.63	0.61	13.39	8.37	0.0024	0.000	0.40	0.01	1.98
La	0.02	0.01	0.02	0.02	3.85	0.93	0.69	2.55	11.59	11.60	0.0005	0.019	0.20	0.00	1.20
Ce	0.07	0.06	0.09	0.07	7.55	2.44	2.00	5.34	26.13	28.69	0.0004	0.002	0.62	0.01	1.01
Pr	0.01	0.01	0.01	0.00	0.99	0.43	0.32	0.76	3.72	4.43	0.0001	0.000	0.12	0.00	0.38
Nd	0.04	0.03	0.06	0.02	4.06	2.15	1.47	3.25	16.85	21.26	0.0004	0.001	0.70	0.01	0.97
Sm	0.02	0.01	0.03	0.01	0.83	0.55	0.33	0.78	3.96	4.89	0.0008	0.000	0.26	0.00	1.17
Eu	0.01	0.01	0.01	0.00	0.37	0.18	0.11	2.42	1.52	1.81	0.0001	0.001	0.10	0.00	1.12
Gd	0.03	0.02	0.04	0.01	0.94	0.53	0.34	0.83	4.43	5.03	0.0004	0.000	0.40	0.01	1.43
Tb	0.01	0.00	0.01	0.00	0.15	0.08	0.06	0.11	0.67	0.73	0.0002	0.000	0.08	0.00	1.12
Dy	0.04	0.03	0.07	0.01	0.89	0.46	0.34	0.74	3.74	3.98	0.0004	0.000	0.54	0.01	1.28
Ho	0.01	0.01	0.02	0.00	0.19	0.10	0.08	0.12	0.75	0.79	0.0001	0.000	0.12	0.00	1.74
Er	0.04	0.03	0.07	0.01	0.53	0.27	0.21	0.38	1.92	2.00	0.0002	0.000	0.35	0.00	1.24
Tm	0.01	0.01	0.01	0.00	0.08	0.05	0.04	0.06	0.29	0.29	0.0001	0.000	0.06	0.00	1.95
Yb	0.06	0.04	0.09	0.01	0.53	0.30	0.23	0.41	1.72	1.73	0.0001	0.000	0.37	0.01	1.73
Lu	0.01	0.01	0.02	0.00	0.08	0.05	0.04	0.06	0.25	0.24	0.0001	0.000	0.06	0.00	0.71
Modal composition															
Ol%	54.34	53.65	52.95	61.90	14.02	50.70	43.03	27.46							
Opx%	39.30	44.38	39.53	33.57	58.69	40.57	39.56	51.20							
Cpx%	4.97	0.37	5.72	3.81	23.15	5.84	14.86	18.05							
Sp%	1.38	1.61	1.79	0.72	4.14	2.89	2.55	3.30							

The average composition calculated from 6 different analyses during the measurements, standard deviation and RSD% values of the internal peridotite standard GP13, as well as the blank values of each elements were also included. DL: detection limits, stan: standard, Ol: olivine, Opx: orthopyroxene, Cpx: clinopyroxene, Spl: spinel. Mg#: magnesium number (MgO/(MgO + FeO)).
The modal mineralogical compositions of the peridotites were calculated using a least squares linear regression created in the MATLAB software. Ol, Opx and Sp (spinel) compositions used in estimations from Dokuz et al. (2011). The Cpx composition was from Le Roux et al. (2007).

The basaltic rocks are characterized by a narrow range of silica (SiO_2 = 45–47 wt.%), alumina (Al_2O_3 = 21–22 wt.%) and magnesium (MgO = 3–4 wt.%) contents, and Cr and Ni values (Table 1). They show enrichment in large-ion lithophile elements (Rb, Ba) with negative troughs in Th and U on the primitive mantle-normalized multi-element diagram (Dokuz et al., 2011). Ta and Sr show positive anomalies, similar to the Beyçam and Pulur peridotites. In contrast to the REE profiles of the Beyçam samples, the REE contents of the basaltic rocks show a negative profile from Nd to Lu.

6.2. Bulk-rock highly siderophile element (HSE) compositions

We present the HSE abundances for the Beyçam and Pulur peridotites and the two basaltic rock samples in Table 2. Average Os (4.4 ppb), Ir (4.4 ppb), Ru (7.8 ppb) and Pt (7.3 ppb) concentrations for the Beyçam harzburgite are similar to the concentrations of the orogenic peridotites (Os = 4.4; Ir = 4.0, Ru = 7.1, Pt = 8.4 ppb; Reisberg and Lorand, 1995; Lorand et al., 2008), to the average upper mantle Os concentration (3.1 ± 0.3 ppb; Morgan, 1986) and to the calculated

Please cite this article as: Dokuz, A., et al., Geochemistry, Re–Os isotopes and highly siderophile element abundances in the Eastern Pontide peridotites (NE Turkey): Multiple episodes ..., Gondwana Research (2014), http://dx.doi.org/10.1016/j.gr.2013.12.010

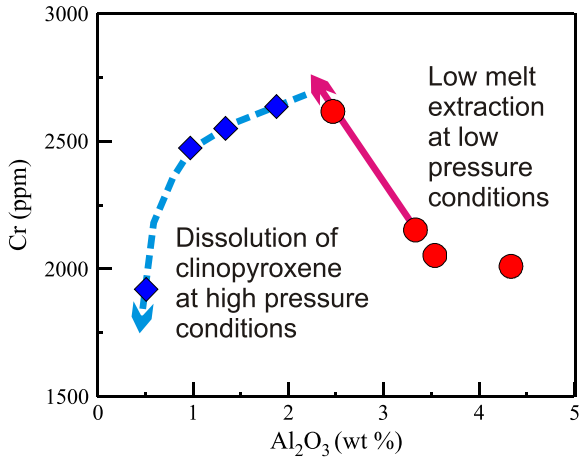

Fig. 5. Al_2O_3 vs. Cr plot showing different co-variations of the Beyçam and Pulur peridotites. Symbols; filled diamond: Beyçam harzburgite, filled circle: Pulur lherzolite.

primitive upper mantle (PUM) Os value (3.9 ± 0.5 ppb; Becker et al., 2006). But, these concentrations are greater than the concentrations of the non-cratonic peridotite xenoliths worldwide (Handler et al., 1999; Meisel et al., 2001; Ackerman et al., 2009). The average concentrations of Pd (2.2 ppb) and Re (0.08 ppb) are ~5 ppb below and ~20 times depleted compared to the average orogenic peridotite values of 8.4 ppb and 1.4 ppb, respectively (Lorand et al., 2008).

Only the average Os concentration (4.7 ppb) for the PL is similar to or slightly greater than both the concentration of the orogenic peridotites (Lorand et al., 2008) and the estimated value for the PUM (Becker et al., 2006). Others, e.g., Ir (2.7 ppb), Ru (5.7) and Pt (6.3 ppb), are generally depleted (~1–2 ppb) relative to those of the PUM values. The Pd concentrations range from 1.1 to 3.3 ppb, with an average value of 2.0 ppb, which is ~5–6 ppb less than the orogenic peridotite and the PUM estimates of 8.4 and 7.1. The Re concentrations (0.05–0.07 ppb) are substantially lower in the Beyçam harzburgite compared to the estimates for the orogenic peridotite (1.43 ppb) and to the PUM values (0.35 ppb) (Becker et al., 2006; Lorand et al., 2008), which are common among those peridotites with a melt depletion history.

Similar to the behavior of Cr (Fig. 5), Os shows different co-variation trends with the fertility indicator Al_2O_3 (Fig. 6). While the Os concentrations in the Beyçam harzburgite are positively correlated, the concentrations in the Pulur lherzolite are negatively correlated with a gentle, curved slope. Different positive slope gradients are also shown in the figure for the Re concentrations. At a given Al_2O_3 content, the Beyçam harzburgite tends to have a greater Re concentration compared with the Pulur lherzolite. For the other HSE of the Pulur lherzolite, the negative correlations are identical, whereas the Beyçam harzburgite do not show such good correlations, except Ir, which is negatively correlated. Consequently, the Re/Os ranges from 0.1141 to 0.2880 for all the peridotite samples, and these values are generally lower than the chondritic Re/Os ratios of 0.406 (Shirey and Walker, 1998) and 0.285 (Horan et al., 2003).

The chondrite-normalized HSE abundances are shown in Fig. 7. These HSE abundances exhibit strongly fractionated patterns for both the Beyçam harzburgite and the Pulur lherzolite samples with enrichments in Os, Ir and Ru. A slight negative Ir anomaly and steeply sloping patterns from Ru to Re are characteristic of the Pulur lherzolite, whereas the Beyçam harzburgite displays flat to slightly depleted Os profiles for the first three elements.

6.3. Re–Os isotopes

The whole-rock $^{187}Os/^{188}Os$ ratios range from 0.1190 to 0.1207 in the Beyçam harzburgite that are less than the present day PUM composition ($^{187}Os/^{188}Os$ = 0.12897, Meisel et al., 2001; Becker et al., 2006), and less than the present day mean chondrite $^{187}Os/^{188}Os$ value of 0.127 (Shirey and Walker, 1998). But, they are within the range of isotopic compositions reported for non-cratonic mantle xenoliths ($^{187}Os/^{188}Os$ = 0. 11541 to 0.12970; Ackerman et al., 2009; Harvey et al., 2010) and for the sub-continental lithospheric mantle ($^{187}Os/^{188}Os$ = 0. 11879 to 0.13454; Meibom et al., 2002; Walker et al., 2002). The $^{187}Re/^{188}Os$ is in the range of 0.0787 to 0.1147, and shows no distinct correlation with Al_2O_3 (Fig. 8a) or $^{187}Os/^{188}Os$ (Fig. 8b); therefore, these values yield no meaningful information for an isochron age.

Some of the distinctive features of the Pulur lherzolite include the greater $^{187}Os/^{188}Os$ (0.1247–0.1315) and generally smaller $^{187}Re/^{188}Os$ (0.04590–0.08341) than the Beyçam harzburgite values. With one exception (sample YS-3C), the $^{187}Os/^{188}Os$ ratios are generally very close to those of the PUM. Sample YS-3C has a $^{187}Os/^{188}Os$ less than that of the PUM and even less than the chondrite values.

The concentrations for the two basaltic rock samples range from 0.102 to 0.331 ppb for Re and from 0.009 to 0.014 ppb for Os, which are within the range of the previously reported MORB glass values (Re = 0.44–2988 ppb, Os = 0.09–31.82 ppb; Hauri and Hart, 1997; Schiano et al., 1997; Escrig et al., 2005; Gannoun et al., 2007). The basaltic rock samples have the $^{187}Os/^{188}Os$ ratios of 0.357 and 1.455, which are greater than the average MORB value of 0.137; however, the $^{187}Re/^{188}Os$ (37.36 and 207.97) is significantly below those of the MORB (e.g., $^{187}Re/^{188}Os$ range from 781 to 2382; e.g., Gannoun et al., 2007). These samples, together with the BH, define a good regression line with a slope corresponding to an age of 376 ± 8.77 Ma with a MSWD value of 0.119 (Fig. 8c). This regression line meets the MSWD

Table 2
Measured HSE abundances (ppb) in the Beyçam and Pulur peridotites and in two basaltic rocks. The T_{RD} and T_{MA} model ages (Walker et al., 1989) were calculated using the GEODATE software program.

	Os	Ir	Ru	Pt	Pd	Re	$^{187}Re/^{188}Os$	$^{187}Os/^{188}Os$	T_{RD}	T_{MA}
Beyçam harzburgite										
BY-8	4.433	4.363	7.389	7.611	1.833	0.073	0.079	0.121	1029.4	1278.4
BY-9	3.842	4.439	6.413	5.076	0.954	0.048	0.079	0.121	985.2	1223.7
BY-11	6.203	4.136	8.027	9.736	4.859	0.148	0.115	0.121	1044.1	1457.9
BY-12	3.193	4.614	9.180	6.753	1.279	0.057	0.086	0.119	1279.1	1624.5
Pulur lherzolite										
YS-3C	4.190	2.172	4.738	4.580	1.879	0.073	0.083	0.125	437.5	552.0
YS-4	5.819	3.595	7.355	5.425	1.082	0.055	0.046	0.129	−130.1	−147.0
YS-7	4.489	2.782	6.014	10.036	3.280	0.052	0.056	0.132	−582.1	−676.3
YS-9	4.508	2.429	5.092	4.990	1.702	0.054	0.058	0.129	−1023.9	−1197.7
Meta-basalt (from Beyçam)										
B-5	0.014	0.018	0.075	0.263	0.141	0.102	37.355	0.357	0	371.4
B-10	0.009	0.020	0.040	0.230	0.040	0.331	207.971	1.455	−50985	382.6

Please cite this article as: Dokuz, A., et al., Geochemistry, Re–Os isotopes and highly siderophile element abundances in the Eastern Pontide peridotites (NE Turkey): Multiple episodes ..., Gondwana Research (2014), http://dx.doi.org/10.1016/j.gr.2013.12.010

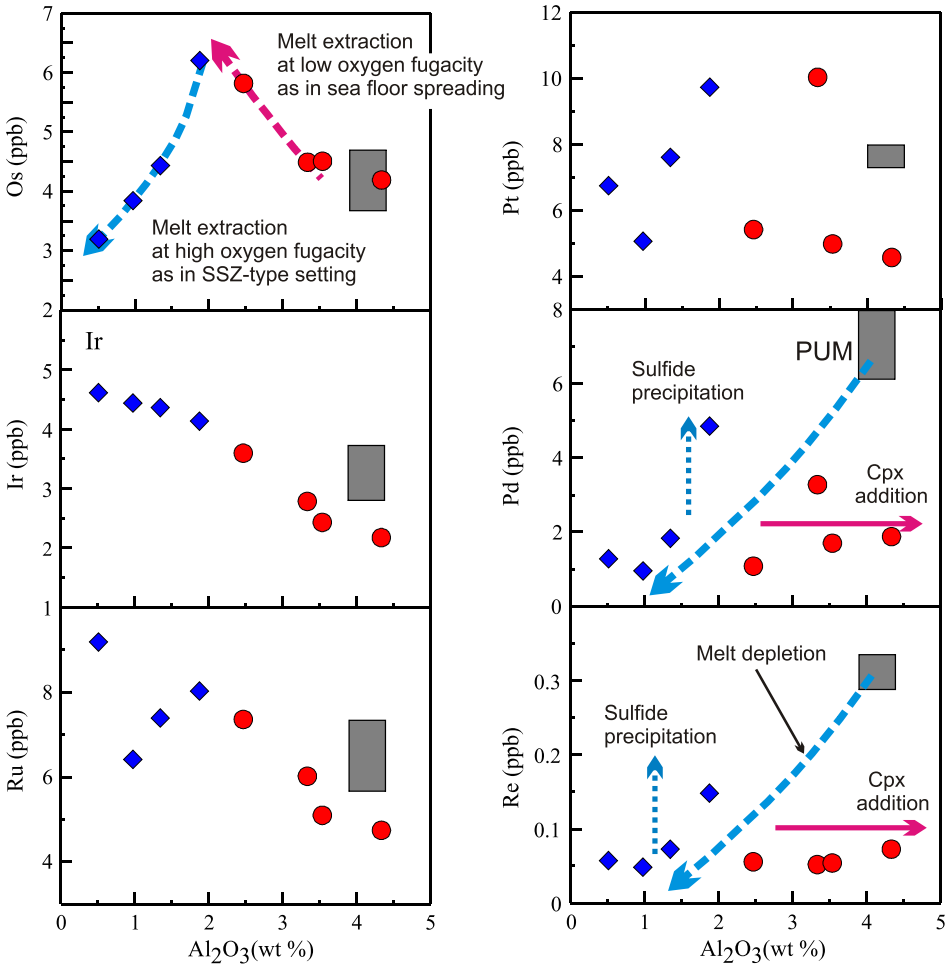

Fig. 6. Variations of HSE vs. Al_2O_3. Primitive upper mantle (PUM) estimates from Becker et al. (2006) and McDonough and Sun (1995). Symbols are as in Fig. 5.

value of 0.119, which does not exceed the maximum expected value of 1.6 (Wendt and Carl, 1991). The obtained isochron age is also consistent with the age constraints obtained from the regional metamorphic rocks (Topuz et al., 2007) and the high-K granitoids (Dokuz, 2011) of the Variscan crystalline basement.

6.4. Role of serpentinization in HSE budget and Os isotope compositions

Roughly constant Ru/Ir, Pd/Ir and Os/Ir ratios in the slightly to extensively serpentinized Pulur lherzolite (Fig. 9) (4–11% LOI) suggest that serpentinization did not significantly affect the Os, Ir, Ru and Pd abundances (Reisberg and Lorand, 1995; Meisel et al., 1996; Büchl et al., 2002; Reisberg et al., 2005; Becker et al., 2006; van Acken et al., 2008; Ackerman et al., 2009; van Acken et al., 2010). Although the slightly positive covariation of compatible HSE (Os, Ir and Ru) with LOI (4–11%; not shown) implies that serpentinization slightly affected the Os, Ir and Ru abundances (Reisberg and Lorand, 1995; Meisel et al., 1996; Büchl et al., 2002; Reisberg et al., 2005; Becker et al., 2006; van Acken et al., 2008; Ackerman et al., 2009; van Acken et al., 2010), negative correlation of these elements with the fertility indicator Al_2O_3 demonstrates that this phenomenon is due to the pyroxene precipitation from a basaltic melt, depleted in terms of HSE similar to the Beyçam Harzburgite, rather than serpentinization. In the case of the Beyçam harzburgite, Os, Pt, Pd and Re show negative correlations with an increasing degree of serpentinization that are in contrast with the addition of significant HSE from the seawater. If a sufficient amount of Os and Re addition had occurred from the seawater, the expected trends would have been positive, indicating that the HSE abundances and ratios were controlled by the primary igneous processes. Furthermore, the Beyçam harzburgite possesses subchondritic $^{187}Os/^{188}Os$ (Fig. 8a) within a narrow range, compared to the ranges observed in the Pulur lherzolite. This is expected, as there is a mantle residue after moderate degrees of partial melting. Conversely, the $^{187}Re/^{188}Os$ of the Beyçam harzburgite was shifted to greater values, compared with those of the Pulur lherzolite (Fig. 8b). This effect might have resulted from a recent Re addition, which may have involved either recrystallization or diffusion, rather than being a primary mantle feature. Thus we do not think that serpentinization may have caused a significant loss on the HSE budget and the Os isotope composition of the mantle residues, and we hence infer that the pre-serpentinization abundances of HSE and isotope compositions are retained in the actual bulk-rock analyses.

7. Beyçam harzburgite: a metasomatized mantle residue

Based on the chromium number of its spinels, Dokuz et al. (2011) have suggested that the Beyçam harzburgite is a mantle residue, produced by moderate amounts (15–20%) of melt extraction. We infer that the first melt-extraction occurred at the spinel stability field beneath a mid ocean ridge spreading center in the early stages of oceanic lithosphere formation subsequent to the continental break up. Then, following the initiation of an intra-oceanic subduction in the Rheic Ocean, a second mantle depletion event occurred in the garnet stability field. Our findings in this study, together with the previous work by Dokuz et al. (2011), support this inference and indicate that, unlike the Pulur lherzolite, the Beyçam harzburgite has mineralogical and geochemical features identical to those of residual peridotites in a mantle wedge.

Please cite this article as: Dokuz, A., et al., Geochemistry, Re–Os isotopes and highly siderophile element abundances in the Eastern Pontide peridotites (NE Turkey): Multiple episodes ..., Gondwana Research (2014), http://dx.doi.org/10.1016/j.gr.2013.12.010

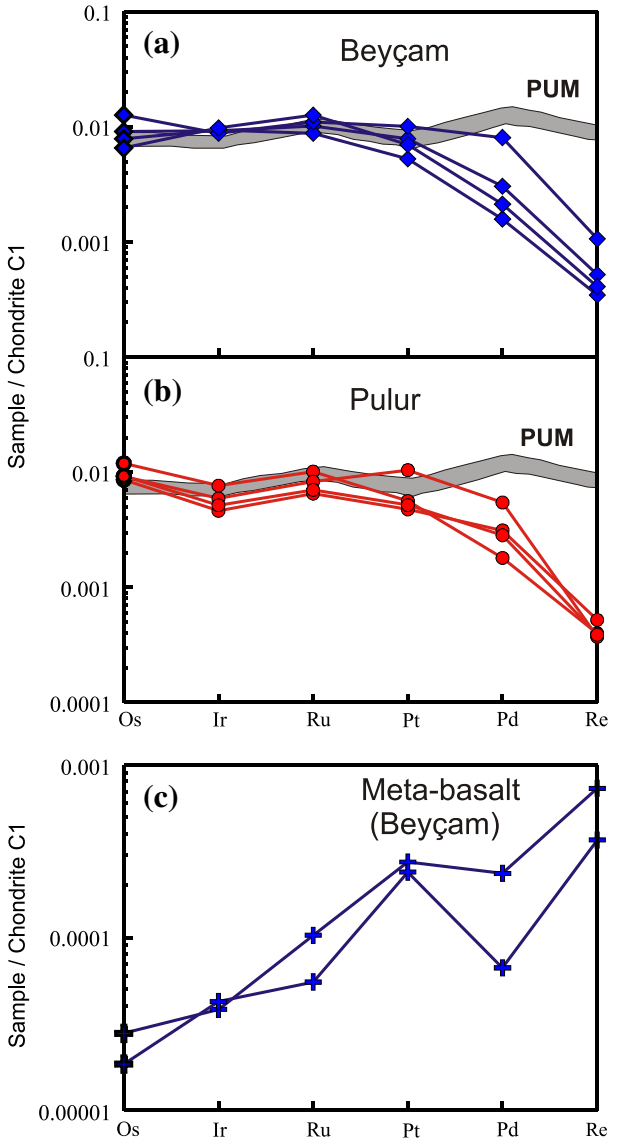

Fig. 7. C1 Chondrite-normalized (average orqueil values from Horan et al., 2003) HSE abundances in the whole rock samples from the (a) Beyçam and (b) Pulur peridotites, and (c) basalt. PUM compositional field is from Becker et al. (2006).

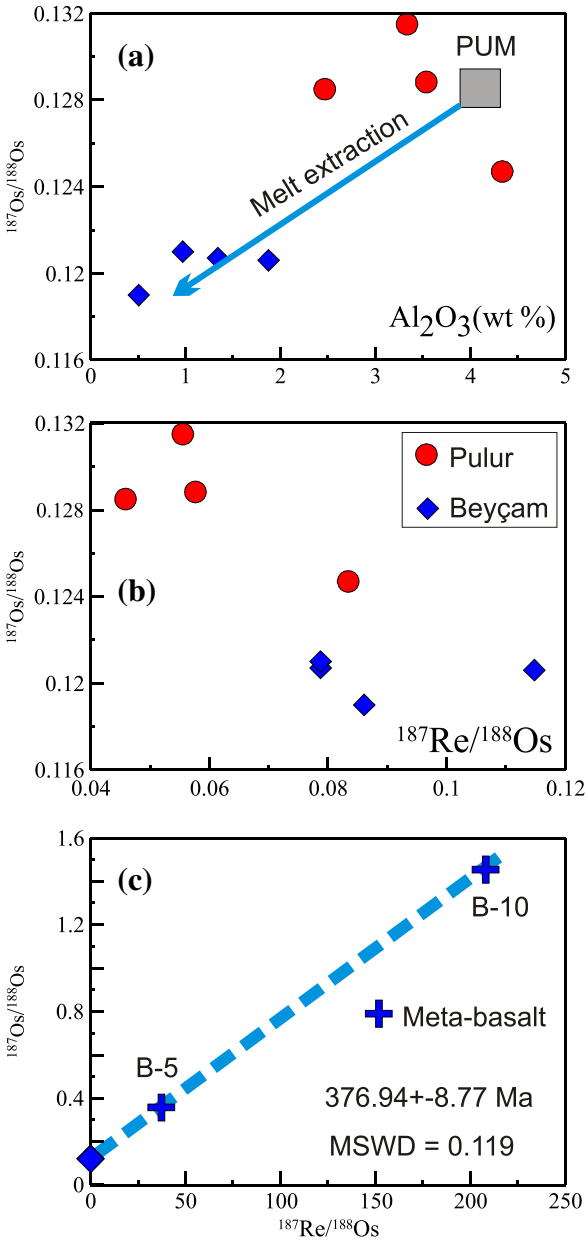

Fig. 8. a. $^{187}Os/^{188}Os$ vs. Al_2O_3 contents of the Beyçam and Pulur samples. Os isotopic ratios of all samples from Beyçam are significantly less than the PUM estimates, whereas the Pulur samples are slightly less than or greater than the PUM estimates. b. $^{187}Os/^{188}Os$ vs. $^{187}Re/^{188}Os$ isotope systematics for the Beyçam and Pulur samples. c. $^{187}Os/^{188}Os$ vs. $^{187}Re/^{188}Os$ isochron diagram for the basaltic rocks and harzburgites from the Beyçam area.

Depletion of a mantle by removal of basaltic melt leads to co-variations in modal mineralogy, in bulk-rock major and trace element compositions, and in the fractionation of parent–daughter elements, comprising the radiogenic isotope systems that are crucial for dating melt depletion events in the mantle. However, in such an environment, isotopic and elemental fingerprints of the previous melt depletion events may be obscured by melts and/or fluids derived from deeper parts of the mantle that overprint or completely erase the evidence for these earlier events. In the following sections, we discuss such processes to assess their possible influence on the HSE distributions and the Re–Os isotopic variations in the Beyçam harzburgite.

7.1. HSE evidence for melt depletion and metasomatism

The degree of partial melting is the main process controlling the modal concentrations of HSE-bearing base metal sulfides and the Re–Os isotopic systematics of the sub-oceanic or sub-continental mantle, although subsequent refertilization by percolating basaltic melts may cause significant variations in the HSE abundances (e.g., Pearson et al., 1995; Brandon et al., 1996; Becker et al., 2001; Lorand et al., 2004; Reisberg et al., 2005; Becker et al., 2006; Walker, 2009) and in the Re–Os isotopic ratios (e.g., Shirey and Walker, 1998; Morgan et al., 2001). The HSE behavior during low-to-moderate degrees of partial melting (<15–20%) is not fully understood. However, with the exception of Re, all HSEs are primarily controlled by base metal sulfide (pyrrhotite, pentlandite, chalcopyrite; Alard et al., 2000; Lorand and Alard, 2001; Luguet et al., 2004) or by metal alloys (Burton et al., 2000; Ballhaus et al., 2006), rather than by oxide or silicate minerals. Those found as inclusions of monosulfide solution (Mss) within the silicate minerals are depleted in Pd group PGE (P-PGE; Pt, Pd) and have unradiogenic $^{187}Os/^{188}Os$. On the other hand, Cu-rich sulfides (e.g., chalcopyrite) found on grain boundaries are enriched in P-PGE, but depleted in Ir group PGE (I-PGE; Os, Ir, Ru), and have more radiogenic $^{187}Os/^{188}Os$ (Burton et al., 1999; Alard et al., 2000).

Some HSE concentrations in the Beyçam harzburgite display different distributions from those in the Pulur lherzolite. For example, the

Please cite this article as: Dokuz, A., et al., Geochemistry, Re–Os isotopes and highly siderophile element abundances in the Eastern Pontide peridotites (NE Turkey): Multiple episodes ..., Gondwana Research (2014), http://dx.doi.org/10.1016/j.gr.2013.12.010

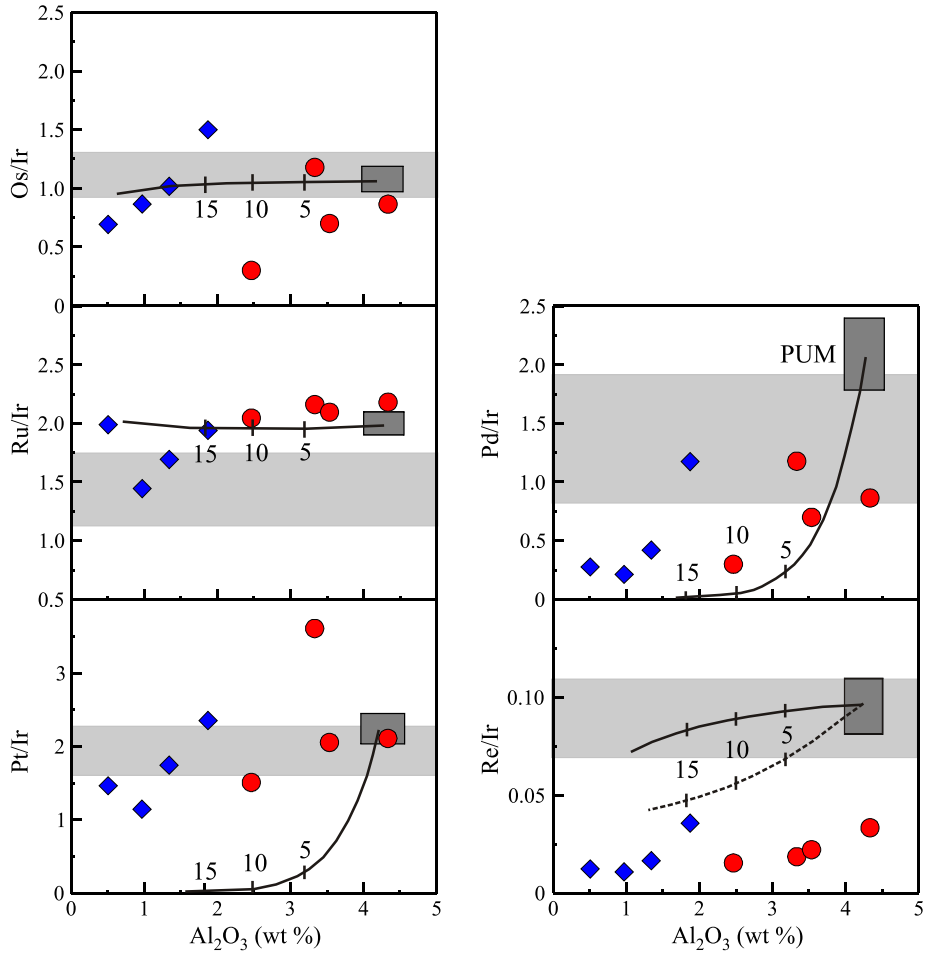

Fig. 9. Os/Ir, Ru/Ir, Pt/Ir, Pd/Ir and Re/Ir vs. Al_2O_3 (wt %). Solid lines: residual peridotite compositions after batch melting, and the dashed line in lower right panel is the residual peridotite composition assuming moderately incompatible bulk partitioning of Re from van Acken et al. (2010). Shaded bar: range of chondritic ratios (Horan et al., 2003). Symbols as in Fig. 5.

Pt, Pd and Re concentrations as well as Pt/Ir, Pd/Ir and Re/Ir ratios in some samples, although moderately depleted, are highly variable but significantly higher than the melt depletion trends and the concentrations we have observed in the samples of the fertile Pulur lherzolite (Figs. 6, 9). This observation is inconsistent with the effects of silicate melt extraction on P-PGE and Re compositions of a residual peridotite, because it requires incremental depletions of these elements in the residue based on the degree of melt extraction. Enrichments of these elements above the melt depletion trends indicate that they would have been added to the residue later. At a low melt–rock ratio, the degree of sulfur saturation of migrating mafic melt and its interaction with the pre-existing, residual mantle sulfide grains strongly affect the HSE budget of the residual peridotite (Mavrogenes and O'Neill, 1999; Bockrath et al., 2004; Brenan et al., 2005). Sulfides and HSE may be removed by sulfur-undersaturated mafic melts from the residual peridotite, whereas sulfur-saturated mafic melts may precipitate sulfides and add HSE to the residual peridotites instead. We infer, therefore, that our HSE data point to Pt, Pd and Re enrichments, which are likely due to a later interaction of the residual peridotite with percolating basaltic melts and to precipitation of the P-PGE enriched interstitial sulfides along the grain boundaries of the silicate phases.

Likewise, the distribution of the Os concentration is striking such that in contrast to Ir, it is positively correlated with the fertility indicator Al_2O_3 (Fig. 6) that involves special environmental conditions wherein Os should be more mobile than Ir. If the Os concentration of the Beyçam harzburgite was only controlled by melt extraction from a lherzolitic protolith, it would have been negatively correlated to Al, as observed for the Ir and Ru, because of its compatible behavior during partial melting (Morgan, 1986; Lorand et al., 1999; Rehkämper et al., 1999a, 1999b; Gannoun et al., 2007). Therefore, the depletion of Os involves its removal from the harzburgitic residue via sulfide breakdown during the subsequent melt–harzburgite reaction. The melt that percolated through the Beyçam harzburgite should have been I-PGE undersaturated mafic melt because it involves an increase in the Os depletion with an increase in the melt–rock reaction.

Additionally, with respect to the chondrite-normalized spidergram (Fig. 7), the depletion of Os relative to Ir is not an expected behavior for the upper mantle residues formed by single-stage partial melting alone. Therefore, Os-depleted PGE patterns and Ir_N/Os_N ratios > 1 are absent from massif peridotites in which sulfides appear to be largely preserved, and from cratonic peridotitic xenoliths that likely contain few primary sulfides (Handler et al., 1999). Conversely, these types of patterns and these large Ir/Os ratios are the features commonly observed in xenoliths brought to the surface by subduction-related magmatism and ascribed to the sulfide breakdown during melt–rock reaction (Handler et al., 1999; Pearson et al., 2004). The role of high oxygen fugacity and the subsequent breakdown of sulfide, which leads to the removal of HSE during volcanic eruptions are discussed by Handler et al. (1999). Based on the experimental solubility data (Wood, 1987) and the physical properties of the oxidized species of these elements, Mungall et al. (2005) have suggested that in a mantle environment with a high oxidation state, Os is more volatile than Ir, and as a result, sulfide dissolution may lead to $Os_N/Ir_N < 1$. Such sulfide dissolution is also likely for the Beyçam harzburgite because a high oxidation state between NNO-2 and NNO has been estimated (Dokuz et al., 2011). The basaltic rock with very low Os (0.003–0.014 ppb) contents is a good

Please cite this article as: Dokuz, A., et al., Geochemistry, Re–Os isotopes and highly siderophile element abundances in the Eastern Pontide peridotites (NE Turkey): Multiple episodes ..., Gondwana Research (2014), http://dx.doi.org/10.1016/j.gr.2013.12.010

candidate for the composition of the inferred basaltic melt that percolated through the harzburgite (Fig. 7c). Depletion in the Al_2O_3 concentrations demonstrates dissolution of some of the pyroxene into the melt during the melt percolation at low melt–rock ratios. Because this process enables the removal of I-PGE-enriched Mss from the pyroxenes, it explains the Os depletion in the samples, as well. These observations also indicate that percolating melt should have been derived from a deeper mantle column that was more depleted as a result of the earlier melt extractions.

7.2. Re–Os isotopic evidence for melt depletion and metasomatism

The Beyçam harzburgite is characterized by a significantly lower $^{187}Os/^{188}Os$ than the chondrite that is consistent with its melt extraction history. The linear correlation between the index of melt depletion (Al_2O_3) and the $^{187}Os/^{188}Os$ also implies that the Beyçam harzburgite remained as a solid residue left behind from partial melting of the Pulur lherzolite—as a starting composition (Fig. 8a). However, if the Beyçam harzburgite represents a mantle residue after a single-stage of melt depletion from a homogeneous starting composition, the Re–Os systematics would have yielded a positive linear correlation corresponding to an isochron age (Walker et al., 1989). There is no such positive linear correlation between the $^{187}Os/^{188}Os$ and $^{187}Re/^{188}Os$ (Fig. 8b). Thus the Os isotopes were either disturbed by an ancient variable melt depletion event or were affected by some other processes subsequent to the latest melt depletion (e.g., Re addition and/or Os loss during melt percolation). Numerous studies (Büchl et al., 2002, 2004; Lorand et al., 2004; Reisberg et al., 2005) have shown that removal of primary (with a low $^{187}Os/^{188}Os$) sulfides and then precipitation of sulfides-bearing radiogenic Os during melt percolation could lead to significant changes in the Os isotopic compositions of the affected peridotites. The latter option is unlikely for the Beyçam harzburgite because of the very low bulk-rock $^{187}Os/^{188}Os$ (0.1190–0.1207). To sufficiently reduce the bulk-rock $^{187}Os/^{188}Os$ to approximately half of that of the fertile mantle (~0.0065), the sulfide grains containing large amounts of Os must also be removed at least in part. A positive correlation between Re and Os, although slightly disturbed, suggests that some Os within the sulfides, enclosed by silicate grains, should have been removed. The interaction with such a melt under oxidizing conditions may have led to the dissolution of primary sulfides (including unradiogenic $^{187}Os/^{188}Os$) within the silicate grains.

8. Pulur lherzolite: a case for mantle refertilization

As shown by recent studies (Le Roux et al., 2007; Rampone et al., 2008; van Acken et al., 2008), varying degrees of partial melting is not the only cause of compositional variability in the lithospheric mantle. Subsequent melt–peridotite interaction can also play a variable role based on the composition of the interacting melt. For instance, asthenosphere-derived, olivine-saturated melts are not in equilibrium with the upper mantle peridotites, and they therefore dissolve pyroxenes and precipitate olivine during their upward migration (Kelemen et al., 1995; 1997). Removal of basaltic melt causes modal and bulk-chemical depletion in the lithospheric mantle and results in the formation of replacive dunites. This is achieved by a dramatic decrease in the contents of pyroxene compatible elements such as Al_2O_3, CaO and Na_2O (melt depletion). Conversely, interaction between the pyroxene-saturated mafic melt and the previously depleted peridotite at low melt–rock ratio leads to a very different manifestation of mantle metasomatism. Precipitation of pyroxenes and sulfides from the mafic melt in harzburgites during this process results in the formation of lherzolite and in an increase in the contents of previously-depleted clinopyroxene compatible elements (refertilization). Examples of such refertilization processes have been reported from abyssal peridotites (Seyler et al., 2007) and peridotite massifs, e.g., Lherz (Le Roux et al., 2007), Totalp (van Acken et al., 2008), Ligurian Alps (Rampone et al., 2004), Mt. Maggiore (Rampone et al., 2008) and Horoman-Japan (Saal et al., 2001; Toramaru et al., 2001), that all preserve ample textural and structural evidence for refertilization. Le Roux et al. (2007) and van Acken et al. (2008) have reported that influxes of LREE-depleted melts under conditions of the asthenosphere–lithosphere transition could lead to transformation of harzburgitic mantle into lherzolite.

Based on the very low Cr-number (5–25) of spinels, Dokuz et al. (2011) have interpreted the Pulur lherzolite as the remnant of a relatively fertile abyssal peridotite, formed by very low-degrees of melt extraction (Arai, 1994). However, field and microscopic observations as well as electron microprobe and whole-rock geochemical data point out that this fertile composition was then modified by melt–rock reactions in a mantle wedge within a suprasubduction zone setting. It is well known that clinopyroxene is a mineral phase that is consumed rapidly during partial melting (Kelemen et al., 1995). Therefore, the repeated events of melt extraction of smaller proportions produce a range of mineral modal abundance in the mantle residue. The calculated clinopyroxene modal abundances of the Pulur lherzolite display a large range (5.8–23.1 modal %), suggesting variable degrees of melt depletion. Conversely, such modal clinopyroxene variations may have originated from refertilization of depleted peridotites through an addition of up to 10% basaltic melt (Elthon, 1992; Beyer et al., 2006).

8.1. Inferences from structural and textural data

The absence of any harzburgite in the Pulur lherzolite precludes the formation of this lherzolite by the mixing of a refractory harzburgite with variable proportions of websterite or pyroxenite. Accordingly, the primary magmatic phases of the Pulur lherzolite have the chemical features typical for a fertile abyssal lherzolite formed by low-degrees (<10%) of partial melting (Dokuz et al., 2011). However, clinopyroxene modal abundances of >15% and a wide range of major-element contents indicate that following this melting process, the primary lherzolitic residue was modified by the addition of some clinopyroxene from a basaltic melt. The addition of basaltic material into the lherzolite is evidenced by the networks of clinopyroxene veins (now replaced by hornblende) that are crosscut by and/or parallel to the planar foliations in the rock (Fig. 2b). The major question here is whether these veins originally formed as clinopyroxene veins in the upper mantle during the melt–rock interaction or later at the crustal level as a result of the Variscan metamorphism.

We analyzed some amphiboles in the hornblendite veins in the Pulur lherzolite. These amphiboles are magnesio-hornblende in composition and are easily distinguished from the other hornblende occurrences by their smaller Mg-number (Fig. 4a). A much smaller Mg-content has been measured in the amphiboles of the basaltic rocks from the Beyçam harzburgite that are mostly Fe-tschermakite in composition (Fig. 4a). This progressive reduction in the Mg-content of the amphiboles, while the corresponding Al-content increases, from lherzolite through hornblendite to basalt (Fig. 4b) indicates that hornblendite and basaltic rocks may have originated from the same parental magmas derived from partial melting of lherzolitic peridotite, similar to the Pulur lherzolite in composition. These magmas were then modified by segregation of the high Mg-bearing phases during their ascent.

No relict clinopyroxene is measured, whereas relict olivine and orthoproxene, and fairly common magnesio-hornblende have been identified in the Pulur lherzolite. The lack of clinopyroxene, which is generally more common in the lherzolite than in the harzburgite, can be explained by the transformation of clinopyroxene to the magnesio-hornblende during the orogenic Variscan metamorphic reactions. The absence of plagioclase, which commonly accompanies hornblende and clinopyroxene in magmatic processes at crustal levels, suggests that the silicate phase precipitated in the lherzolite from the percolating basaltic melt channels was clinopyroxene, not hornblende. Furthermore, the lack of high-pressure minerals (i.e. garnet), suggests that the

Please cite this article as: Dokuz, A., et al., Geochemistry, Re–Os isotopes and highly siderophile element abundances in the Eastern Pontide peridotites (NE Turkey): Multiple episodes ..., Gondwana Research (2014), http://dx.doi.org/10.1016/j.gr.2013.12.010

refertilization processes occurred at shallow mantle depths, in the uppermost section of the mantle wedge (i.e., spinel lherzolite). The refertilized samples show no interference between the parts of clinopyroxenite vein and the lherzolite, suggesting that the melt–rock reaction was restricted to the wall space of the clinopyroxenite veins, and that the mixing processes responsible for the chemical variations in the Pulur lherzolite occurred at a solid-state.

8.2. Inferences from the HSE distributions

Cu-rich sulfides are partially to completely removed, prior to dissolution of Mss, during low-degrees of mantle melting (Bockrath et al., 2004). This commonly leads to a selective enrichment in Os, Ir and Ru, and to depletion in Pt and Pd concentrations of melt residues. The Pt, Pd and Re concentrations of the Pulur lherzolite are variably depleted relative to those of the PUM (Fig. 6), consistent with a mantle residue formed by low-degrees (<10%) of melt extraction. This inference is favored by the progressive increase of the Os, Ir and Ru contents, which are compatible at low degrees of melting, with a negative trend passing above the PUM field. However, the low degrees of partial melting alone are not capable of reducing the Ir-group PGE concentrations in residues below those concentrations of the PUM that once existed in their precursor. As Fig. 9 shows, the Os/Ir ratios are less than those of the PUM and are positively correlated with the Al_2O_3 contents. These observations are inconsistent with the notion of partial melting as a single process during the formation of the Pulur lherzolite. Therefore, these rocks must have involved at least one additional process, such as refertilization or melt–mantle reaction, which is capable of decreasing the I-PGE values below those of the PUM.

An interaction between a HSE-saturated silicate melt and a mantle peridotite at a low melt–rock ratio can be ruled out because such a process commonly results in the precipitation of interstitial sulfides, which are rich in P-PGE (Becker et al., 2001; Saal et al., 2001; Luguet et al., 2004). Conversely, the moderately depleted P-PGE concentrations of the Pulur lherzolite are consistent with the percolation of an HSE-undersaturated melt because such a melt can cause dissolution of some sulfides, and may consequently result in the removal of certain HSE from the affected rock (e.g., Lorand and Alard, 2001; Lorand et al., 2004; Reisberg et al., 2005). Parts of the Pulur lherzolite, in which clinopyroxene-rich channels and veins predominate, represent the products of a solid-state mixing process, which took place during the formation of the lherzolitic residue. This is because the concentration of I-PGE in the refractory lherzolite is likely to be several orders of magnitude higher, whereas Al_2O_3 abundances are an order of magnitude lower, than those of the melt. In this context, the basaltic rocks from the Beyçam area provide important information about the nature of the silicate melt, which interacted with the Pulur and Beyçam peridotites. As observed in the chondrite-normalized spidergram (Fig. 7), the basalt samples display positive slopes of HSE with enrichment in P-PGE and Re. However, the absolute abundances of the I-PGE and even the P-PGE and Re are lower than those of their probable residual precursor (Pulur lherzolite), indicating that the interacting melt might have been HSE-undersaturated. This inference contradicts with the Mss/sulfide melt distribution coefficients of ~0.01–0.1 for Pt and Pd and ~2–3 for Re during partial melting (Barnes et al., 1997; Ballhaus et al., 2006). Therefore, the depleted P-PGE values of the basaltic samples suggest that the refractory peridotite should have been depleted as a result of the production of previous melts of basaltic compositions.

Rhenium is coherent with, but generally more depleted than, Pd and Pt in the Pulur lherzolite (Figs. 6 and 9); this Re behavior is not in agreement with the Dmss/sulfide distribution coefficients. Rhenium is the most lithophilic element among the HSE and becomes incorporated into silicate minerals, particularly into the clinopyroxene, during partial melting (Righter and Hauri, 1998; Sattari et al., 2002; Fonseca et al., 2007; Mallmann and O'Neill, 2007). Therefore, the addition of such clinopyroxene-rich melt to the residual lherzolite with a large I-PGE content would cause a reduction in the I-PGE contents to the levels that are significantly less than those of their source. This process would create curved mixing arrays on the plots of Al_2O_3 vs. I-PGE (Reisberg and Lorand, 1995), as observed in the Os and Re distributions of our samples. This process also explains the P-PGE contents of those samples plotting in the right side of the melt-depletion trends (Fig. 6), and the Re/Ir ratios that are less than partial melting trends (Fig. 9) because of the addition of a melt with Al_2O_3 abundances greater than an order of magnitude. An increase of Pt/Ir above the melting trends may indicate the precipitation of a Pt-bearing sulfide phase during the melt–peridotite interaction.

8.3. Inferences from Re–Os systematics

The bulk-rock Os isotope ratios of the Pulur lherzolite are highly variable. With one exception (Sample YS-3C), the suprachondritic $^{187}Os/^{188}Os$ ratios, one of which is even higher than that of PUM, are inconsistent with melt depletion ($^{187}Os/^{188}Os_{chondrite} = 0.127$; Shirey and Walker, 1998). Although not very distinct, the negative correlations between the $^{187}Os/^{188}Os$ and $^{187}Re/^{188}Os$ and the Al_2O_3 contents (Fig. 8a, b) suggest that these values may have been perturbed by other processes subsequent to the melt depletion. If the Os isotope ratios were controlled by simple in-growth of ^{187}Os from Re, a positive co-variation would have shown. Moreover, Sample YS-3C displaying the greatest Re content would have had the greatest $^{187}Os/^{188}Os$. This sample is the richest in modal clinopyroxene that was precipitated during solid-state melt–rock interaction. Nevertheless, the lack of variation in the $^{187}Os/^{188}Os$ can be explained by non-precipitation of radiogenic Os-bearing sulfides, whereas clinopyroxene was precipitated from a basaltic melt causing the reduction of the modal amount of pre-existing sulfide in the rock. Conversely, the supra-PUM values of the $^{187}Os/^{188}Os$ suggest that the bulk-rock Os budget may have been disturbed after melt depletion, either by an addition of radiogenic Os, or through Re addition and subsequent in-growth of ^{187}Os. Taking the basaltic rocks with very radiogenic $^{187}Os/^{188}Os$ into account, the addition of radiogenic Os appears to be a more plausible explanation for the increase in the Os to radiogenic levels.

9. Melt depletion and isochron ages

Because of the addition of some radiogenic Re- and Os-bearing phases into the peridotites, the isotopic system established during the first melt-extraction was disturbed (Fig. 8a). Therefore, together or separately no obvious isochronous relationships exist for the Pulur and Beyçam peridotites (Fig. 8b). This scatter is generally ascribed to Re mobility because Re behaves very mobile, whereas Os immobile, under a wide range of conditions such as low to moderate partial melting, and melt–rock reaction either at high or low melt/rock ratios (e.g., Reisberg and Lorand, 1995; Kelemen et al., 1997; Meisel et al., 2001; Sun et al., 2003). In such a case, if Re has been added or removed, useful information on the last melt extraction event can be obtained by individual model rhenium-depletion (T_{RD}) ages, because this approach ignores the in-growth of ^{187}Os (Walker et al., 1989; Shirey and Walker, 1998). Individual model T_{RD} ages range between the future and 437 Ma for the Pulur lherzolite and between 0.98 and 1.27 Ga for the Beyçam harzburgite (Table 2). Given that both the lherzolite and harzburgite are the vestiges of the Rheic oceanic mantle, which evolved between the late Cambrian and the early Carboniferous (Murphy et al., 2010; Nance et al., 2010), the T_{RD} model ages from both suites appear to have diverged from each other by a subsequent process. We infer that this divergence was due to Re loss in the Pulur lherzolite and Re gain in the Beyçam harzburgite.

Conversely, the melt of the basaltic rocks appears to have escaped the subsequent metasomatic events as it ascended within the mantle wedge. The two basaltic samples, along with the samples of the Beyçam harzburgite, form an isochron on the plot of $^{187}Re/^{188}Os$ vs. $^{187}Os/^{188}Os$

Please cite this article as: Dokuz, A., et al., Geochemistry, Re–Os isotopes and highly siderophile element abundances in the Eastern Pontide peridotites (NE Turkey): Multiple episodes ..., Gondwana Research (2014), http://dx.doi.org/10.1016/j.gr.2013.12.010

corresponding to an age of 377 ± 8.77 Ma (Fig. 8c) that places these rocks in the Paleozoic Rheic Ocean realm (Kroner et al., 2007). A further constraint on the time of melt extraction from the Rheic mantle wedge can be drawn from the T_{MA} model age (Walker et al., 1989) that is the measure of the length of time during which a melt has been separated from the mantle as an analog to the T_{DM} model age calculations (DePaolo and Wasserburg, 1976). The calculated T_{MA} ages of 371.4 Ma and 382.6 Ma for the basaltic samples (Table 2) are hence insightful as they are within the range of error of the isochron age described above. Consequently, this isochron age may correspond to the time at which the Beyçam harzburgite was metasomatized by subduction-derived fluids leading to the production of the melt that produced the basaltic rocks by dissolution of the clinopyroxene. Furthermore, this was the time at which the Pulur lherzolite was networked by the channels in which clinopyroxene precipitation occurred. Thus, the calculated T_{DM} and T_{MA} ages from our basaltic rock samples may provide a minimum age constraint for the timing of subduction initiation and related fluid flux in the mantle wedge of a Rheic subduction zone.

10. Conclusions

The Paleozoic Variscan peridotites from the eastern part of the Sakarya Zone (Turkey) demonstrate a composite mantle lithosphere evolution, characterized by partial melting and subsequent multi-stage melt migration and melt–rock interactions. The Pulur lherzolite was produced by low-degrees of melt depletion in the spinel stability field that is typical for those of fertile abyssal-type lherzolites. The dissolution of the remaining pyroxene, spinel and sulfide minerals in the garnet stability field in a suprasubduction zone setting resulted in the formation of a moderately depleted harzburgitic residue (Beyçam harzburgite) and basaltic daughter melt. Partial interaction between the harzburgite and this basaltic melt led to enrichment in the concentrations of incompatible HSE (Pd, Pt) and Re of the Beyçam harzburgite. Another melt–peridotite interaction occurred in the upper level of the mantle wedge between the basaltic melt and the earlier formed abyssal lherzolite. This interaction likely occurred in a mechanical state by precipitation of clinopyroxene, spinel and sulfides from the basic melt in the veins and channels of the Pulur lherzolite. Large negative covariations of the compatible HSE (Os, Ir and Ru) with the fertility indicator Al_2O_3 are a consequence of this type of interaction, rather than variable melt extraction. Island arc tholeiite-type basaltic rocks in the Beyçam area, along with their HSE distributions typical for a basaltic melt originated from a harzburgitic mantle residue, represent this inferred percolating basaltic melt. The Re–Os isochron age of 377 ± 8.77 Ma of the basaltic rocks indicates that these peridotites and basaltic rocks represent the relics of the Rheic oceanic lithosphere.

Supplementary data to this article can be found online at http://dx.doi.org/10.1016/j.gr.2013.12.010.

Acknowledgments

Our work in the Eastern Pontides has been supported by research grants from TUBITAK, Turkey. Y Dilek acknowledges the support by the Mineral Research and Exploration Institute of Turkey (MTA) and Miami University (through his Distinguished Professor discretionary funds) for his fieldwork in NE Turkey. Constructive and thorough reviews by J. Brendan Murphy, Mei-Fu Zhou and Jingsui Yang helped us improve the science and organization of the paper, and are gratefully acknowledged. We thank the Gondwana Research Editor-in-Chief, Professor Santosh, and the Special Issue Guest Editors for their editorial handling of the manuscript.

Appendix I. Sample preparation

One hundred milligrams of the powdered sample was added to a Teflon vial along with 4 mL of HF and 1 mL HNO_3 (SPA, ROMIL Cambridge); the vial was sealed and left on a hot plate at 150 °C for 48 h. The acid mixture was allowed to evaporate to near dryness; to the moist residue, 1 mL HNO3 was added, and the mixture was again evaporated to near dryness. A second 1 mL aliquot of HNO3 was added and evaporated to near-dryness. These steps converted the insoluble fluoride species into soluble nitrate species. To the sample, 2.5 mL of $HNO_3$was added and diluted to 50 mL after the addition of an internal standard, which gave a final concentration of 20 ppb of Re and Rh. The internal standard was used to compensate for any analytical drift and matrix-suppression effects.

Calibration of the ICP-MS was assured by using the international rock standards (BHVO-1, AGV-1, W-2, NBS688) with the addition of an in-house peridotite standard (GP13) (Ottley et al., 2003). These standards and analytical blanks were prepared using the same technique as the samples. To improve the signal-to-noise threshold, the low-abundance isotopes were measured with increased dwell times (Ottley et al., 2003). The reference samples (W-2, AGV-1, BHVO-1, BE-N, NBS688 and GP13) were analyzed as unknown samples during the same analytical runs as the Pulur and Beyçam samples. For the elements investigated, the reproducibility of these reference samples was generally greater than 2%, and the measured compositions compared favorably with the compositions published by Potts et al. (1992).

Appendix II. HSE analysis

Two grams of finely powdered samples, with the addition of multi-elemental spike of HSE isotope tracers (^{185}Re, ^{190}Os, ^{101}Ru, ^{106}Pd, ^{191}Ir and ^{198}Pt), were dissolved in a mixture of 5 mL HNO_3 and 2 mL HCl in closed-quartz vials in a High Pressure Asher (HPA) system (Anton Paar-Perkin-Elmer Instruments, Graz) at 300 °C and at a pressure of 125 bar for 4 h. The Os concentration and the Os isotope ratio were measured as the volatile OsO_4 complex, which was directly fed into the quadrupole ICP-MS system (®HP7500 Agilent Technologies). The residue was centrifuged, dried on a hot plate, and re-dissolved in 1.5 mL of 0.1 mol/L HCl. The solution was filtered and introduced into a cation-exchange resin column (Dowex AG50Wx8 200–400 mesh, Fluka) connected directly to the tubing system of the peristaltic pump on the mass spectrometer. The time signal was monitored, and the relevant, overlap-free part of the signal was used to calculate the concentrations. The HSE concentrations from the repeated digestion of the fresh aliquots of the ultramafic reference material (UB-N) were in the compositional range obtained by Meisel and Moser (2004), which indicates an uncertainty of <10%.

References

Ackerman, L., Walker, R.J., Puchtel, I.S., Pitcher, L., Jelnek, E., Strnad, L., 2009. Effects of melt percolation on highly siderophile elements and Os isotopes in subcontinental lithospheric mantle: a study of the upper mantle profile beneath Central Europe. Geochimica et Cosmochimica Acta 73, 2400–2414.

Alard, O., Griffin, W.L., Lorand, J.-P., Jackson, S.E., O'Reilly, S.Y., 2000. Non-chondritic distribution of the highly siderophile elements in mantle sulfides. Nature 407, 891–894.

Alard, O., Griffin, W.L., Pearson, N.J., Lorand, J.-P., O'Reilly, S.Y., 2002. New insights into the Re–Os systematics of sub-continental lithospheric mantle from in situ analysis of sulphides. Earth and Planetary Science Letters 203, 651–663.

Aldanmaz, Meisel, T., Celik, O.F., Henjes-Kunst, F., 2012. Osmium isotope systematics and highly siderophile element fractionation in spinel-peridotites from the Tethyan ophiolites in SW Turkey: implications for multi-stage evolution of oceanic upper mantle. Chemical Geology 294–295, 152–164.

Anbar, A.D., Creaser, R.A., Papanastassiou, D.A., Wasserberg, G.J., 1992. Rhenium in seawater: confirmation of generally conservative behavior. Geochimica et Cosmochimica Acta 56, 4009–4103.

Anderson, D.L., 2006. Peculations on the nature and cause of mantle heterogeneity. Tectonophysics 416, 7–22.

Arai, S., 1994. Characterisation of spinel peridotites by olivine–spinel compositional relationships: review and interpretation. Chemical Geology 113, 191–204.

Ballhaus, C., Bockrath, C., Wohlgemuth-Ueberwasser, C., Laurenz, V., Berndt, J., 2006. Fractionation of the noble metals by physical processes. Contributions to Mineralogy and Petrology 152, 667–684.

Barnes, S.-J., Makovicky, E., Makovicky, M., Rose-Hansen, J., Karup-Moller, S., 1997. Partition coefficients for Ni, Cu, Pd, Pt, Rh, and Ir between monosulphide solid solution and

sulfide liquid and the formation of compositionally zoned Ni–Cu bodies by fractional crystallization of sulide liquid. Mineralogical Magazine 58A, 4881–4888.
Batanova, V.G., Brügmann, G.E., Bazylev, B.A., Sobolev, A.V., Kamenetsky, V.S., Hofmann, A.W., 2008. Platinum-group element abundances and Os isotope composition of mantle peridotites from the Mamonia complex, Cyprus. Chemical Geology 248, 195–212.
Becker, H., Shirey, S.B., Carlson, R.W., 2001. Effects of melt percolation on the Re–Os systematics of peridotites from a Paleozoic convergent plate margin. Earth and Planetary Science Letters 188, 107–121.
Becker, H., Horan, M.F., Walker, R.J., Gao, S., Lorand, J.-P., Rudnick, R.L., 2006. Highly siderophile element compositions of the Earth's primitive mantle. Geochimica et Cosmochimica Acta 70, 4528–4550.
Beyer, E.E., Griffin, W.L., O'Reilly, S.Y., 2006. Transformation of Archean lithospheric mantle by re-fertilization: evidence from exposed peridotites in the Western Gneiss Region, Norway. Journal of Petrology 47, 1611–1636.
Bézard, R., Hébert, R., Wang, C.-S., Dostal, J., Dai, J., Zhong, H., 2011. Petrology and geochemistry of the Xiugugabu ophiolitic massif, western Yarlung Zangbo suture zone, Tibet. Lithos 125, 347–367.
Bockrath, C., Ballhaus, C., Holzheid, A., 2004. Fractionation of the platinum-group elements during mantle melting. Science 305, 1951–1953.
Bodinier, J.L., 1988. Geochemistry and petrogenesis of the Lanzo peridotite body, western Alps. Tectonophysics 149, 67–88.
Bodinier, J.-L., Godard, M., 2003. Orogenic, ophiolitic, and abyssal peridotites. In: Carlson, R.W. (Ed.), Treatise on Geochemistry. Mantle and Core. Treatise on Geochem, vol. 2. Elsevier Science Ltd., pp. 103–170.
Boudier, F., Coleman, R.G., 1981. Cross section through the peridotite in the Samail Ophiolite, southeastern Oman Mountains. Journal of Geophysical Research: Solid Earth 86, 2573–2592.
Brandl, P.A., Beier, C., Regelous, M., Abouchami, W., Haase, K.M., Garbe-Schönberg, D., Galer, S.J.G., 2012. Volcanism on the flanks of the East Pacific Rise: quantitative constraints on mantle heterogeneity and melting processes. Chemical Geology 298–299, 41–56.
Brandon, A.D., Creaser, R.A., Shirey, S.B., Carlson, R.W., 1996. Osmium recycling in subduction zones. Science 272, 861–864.
Brandon, A.D., Norman, M.D., Walker, R.J., Morgan, J.W., 1999. ^{186}Os–^{187}Os systematics of Hawaiian picrites. Earth and Planetary Science Letters 174, 25–42.
Brenan, J.M., McDonough, W.F., Ash, R., 2005. An experimental study of the solubility and partitioning of iridium, osmium and gold between olivine and silicate melt. Earth and Planetary Science Letters 237, 855–872.
Brunelli, D., Seyler, M., Cipriani, A., Ottolini, L., Bonatti, E., 2006. Discontinuous melt extraction and weak refertilization of mantle peridotites at the Vema lithospheric section (Mid-Atlantic ridge). Journal of Petrology 47, 745–771.
Büchl, A., Brügmann, G., Batanova, V.G., Münker, C., Hofmann, A.W., 2002. Melt percolation monitored by Os isotopes and HSE abundances: a case study from the mantle section of the Troodos Ophiolite. Earth and Planetary Science Letters 204, 385–402.
Büchl, A., Brügmann, G., Batanova, V.G., Hofmann, A.W., 2004. Os mobilization during melt percolation: the evolution of Os isotope heterogeneities in the mantle sequence of the Troodos ophiolite, Cyprus. Geochimica et Cosmochimica Acta 68, 3397–3408.
Burnham, O.M., Rogers, N.W., Pearson, D.G., van Calsteren, P.W., Hawkesworth, C.J., 1998. The petrogenesis of the eastern Pyrenean peridotites: an integrated study of their whole-rock geochemistry and Re–Os isotope composition. Geochimica et Cosmochimica Acta 62, 2293–2310.
Burton, K.W., Schiano, P., Birck, J.-L., Allègre, C.J., 1999. Osmium isotope disequilibrium between mantle minerals in a spinel-lherzolite. Earth Planetary Science Letters 172, 311–322.
Burton, K.W., Schiano, P., Birck, J.-L., Allegre, C.J., Rehkämper, M., Halliday, A.N., Dawson, J.B., 2000. The distribution of rhenium and osmium amongst mantle minerals and the age of the lithospheric mantle beneath Tanzania. Earth and Planetary Science Letters 183, 93–106.
DePaolo, D.J., Wasserburg, G.J., 1976. Nd isotopic variation and petrogenetic models. Geophysical Research Letters 3, 249–252.
Dijkstra, A.H., Drury, M.R., Vissers, R.L.M., Newman, J., Van Roermund, H.L.M., 2004. Shear zones in the upper mantle: evidence from alpine- and ophiolite-type peridotite massifs. Geological Society of London, Special Publication 224, 11–24.
Dilek, Y., 2006. Collision tectonics of the Eastern Mediterranean region: causes and consequences. Geological Society of America, Special Paper 409, 1–13.
Dilek, Y., Delaloye, M., 1992. Structure of the Kizildag Ophiolite, a slow-spread Cretaceous ridge segment north of the Arabian Promontory. Geology 20, 1–13.
Dilek, Y., Eddy, C.A., 1992. The Troodos (Cyprus) and Kizildag (S. Turkey) ophiolites as structural models for slow-spreading ridge segments. Journal of Geology 100, 305–322.
Dilek, Y., Flower, M.F.J., 2003. Arch-trench rollback and forearc accretion: a model template for ophiolites in Albania, Cyprus and Oman. In: Dilek, Y., Robinson, P.T. (Eds.), Ophiolies in Earth History. Geological Society of London Special Publication, 218, pp. 43–68.
Dilek, Y., Furnes, H., 2009. Structure and geochemistry of Tethyan ophiolites and their petrogenesis in subduction rollback systems. Lithos 113, 1–20.
Dilek, Y., Furnes, H., 2011. Ophiolite genesis and global tectonics: geochemical and tectonic fingerprinting of ancient oceanic lithosphere. The Geological Society of America Bulletin 123, 387–411.
Dilek, Y., Morishita, T., 2009. Melt migration and upper mantle evolution during incipient arc construction: Jurassic Eastern Mirdita ophiolite, Albania. Island Arc 18, 551–554.
Dilek, Y., Robinson, P.T., 2003. Ophiolites in Earth history: introduction. In: Dilek, Y., Robinson, P.T. (Eds.), Ophiolites in Earth History. Geological Society of London Special Publication, 218, pp. 1–8.
Dilek, Y., Rowland, J.C., 1993. Evolution of a conjugate passive margin pair in Mesozoic Southern Turkey. Tectonics 12, 954–970.
Dilek, Y., Thy, P., 2009. Island arc tholeiite to boninitic melt evolution of the Cretaceous Kizildag (Turkey) ophiolite: model for multi-stage early arc-forearc magmatism in Tethyan subduction factories. Lithos 113, 68–87.
Dokuz, A., 2011. A slab detachment and delamination model for the generation of Carboniferous high-potassium I-type magmatism in the Eastern Pontides, NE Turkey: the Köse composite pluton. Gondwana Research 19, 926–944.
Dokuz, A., Tanyolu, E., 2006. Geochemical constraints on the provenance, mineral sorting and subaerial weathering of Lower Jurassic and Upper Cretaceous clastic rocks from the Eastern Pontides, Yusufeli (Artvin), NE Turkey. Turkish Journal of Earth Sciences 15, 181–209.
Dokuz, A., Karslı, O., Chen, B., Uysal, I., 2010. Sources and petrogenesis of Jurassic granitoids in the Yusufeli area, Northeastern Turkey: implications for pre- and post-collisional lithospheric thinning of the Eastern Pontides. Tectonophysics 480, 259–279.
Dokuz, A., Uysal, I., Kaliwoda, M., Karsli, O., Ottley, C.J., Kandemir, R., 2011. Early abyssal- and late SSZ-type vestiges of the Rheic oceanic mantle in the Variscan basement of the Sakarya Zone, NE Turkey: implications for the sense of subduction and opening of the Paleotethys. Lithos 127, 176–191.
Donnelly, K., Goldstein, S., Langmuir, C., Spiegelman, M., 2004. Origin of enriched ocean ridge basalts and implications for mantle dynamics. Earth and Planetary Science Letters 226, 347–366.
Edwards, S.J., Malpas, J., 1996. Melt–peridotite interactions in shallow mantle at the East Pacific Rise: evidence from ODP Site 895 (Hess Deep). Mineralogical Magazine 60, 191–206.
Elthon, D., 1992. Chemical trends in abyssal peridotites: re-fertilization of depleted suboceanic mantle. Journal of Geophysical Research 97, 9015–9025.
Escrig, S., Schiano, P., Schilling, J.-G., Allègre, C.J., 2005. Rhenium–osmium isotope systematics in MORB from the Southern Mid-Atlantic Ridge (408–508 S). Earth and Planetary Science Letters 235, 528–548.
Eyuboglu, Y., Dilek, Y., Bozkurt, E., Bektas, O., Rojay, B., Sen, C., 2010. Structure and geochemistry of an Alaskan-type ultramafic–mafic complex in the Eastern Pontides, NE Turkey. Gondwana Research 18, 230–252.
Eyuboglu, Y., Santosh, M., Bektas, O., Ayhan, S., 2011. Arc magmatism as a window to plate kinematics and subduction polarity: example from the eastern Pontides belt, NE Turkey. Geoscience Frontiers 2, 49–56.
Flower, M.F.J., Dilek, Y., 2003. Arc-trench rollback and forearc accretion: 1. A collision-induced mantle flow model for Tethyan ophiolites. In: Dilek, Y., Robinson, P.T. (Eds.), Ophiolites in Earth History. Geological Society of London Special Publication, 218, pp. 21–42.
Fonseca, R.O.C., Mallmann, G., O'Neill, H.S.C., Campbell, I.H., 2007. How chalcophile is rhenium? An experimental study of the solubility in sulphide mattes. Earth and Planetary Science Letters 260, 537–548.
Frey, F.A., Suen, C.J., Stockman, H.W., 1985. The Ronda high temperature peridotite: geochemistry and petrogenesis. Geochimica et Cosmochimica Acta 49, 2469–2491.
Gannoun, A., Burton, K.W., Parkinson, I.J., Alard, O., Schiano, P., Thomas, L.E., 2007. The scale and origin of the osmium isotope variations in mid-ocean ridge basalts. Earth and Planetary Science Letters 259, 541–556.
González-Jiménez, J.M., Proenza, J.A., Gervilla, F., Melgarejo, J.C., Blanco-Moreno, J.A., Ruiz-Sánchez, R., Griffin, W.L., 2011. High-Cr and high-Al chromitites from the Sagua de Tánamo district, Mayarí-Cristal ophiolitic massif (eastern Cuba): constraints on their origin from mineralogy and geochemistry of chromian spinel and platinum-group elements. Lithos 125, 101–121.
Handler, M.R., Bennett, V.C., Dreibus, G., 1999. Evidence from correlated Ir/Os and Cu/S for late-stage Os mobility in peridotite xenoliths: implications for Re–Os systematics. Geology 27, 75–78.
Handler, M.R., Bennett, V.C., Carlson, R.W., 2005. Nd, Sr and Os isotope systematics in young, fertile spinel peridotite xenoliths from northern Queensland, Australia: a unique view of depleted MORB mantle? Geochimica et Cosmochimica Acta 69, 5747–5763.
Harvey, J., Gannoun, A., Burton, K.W., Rogers, N.W., Alard, O., Parkinson, I.J., 2006. Ancient melt extraction from the oceanic upper mantle revealed by Re–Os isotopes in abyssal peridotites from the Mid-Atlantic ridge. Earth and Planetary Science Letters 244, 606–621.
Harvey, J., Gannoun, A., Burton, K.W., Schiano, P., Rogers, N.W., Alard, O., 2010. Unravelling the effects of melt depletion and secondary infiltration on mantle Re–Os isotopes beneath the French Massif Central. Geochimica et Cosmochimica Acta 74, 293–320.
Hauri, E.H., Hart, S.R., 1997. Rhenium abundances and systematics in oceanic basalts. Chemical Geology 139, 185–205.
Horan, M.F., Walker, R.J., Morgan, J.W., Grossman, J.N., Rubin, A.E., 2003. Highly siderophile elements in chondrites. Chemical Geology 196, 27–42.
Ishikawa, A., Kaneko, Y., Kadarusman, A., Ota, T., 2007. Multiple generations of forearc mafic–ultramafic rocks in the Timor–Tanimbar ophiolite, eastern Indonesia. Gondwana Research 11, 200–217.
Kandemir, R., Lerosey-Aubril, R., 2011. First report of a trilobite in the Carboniferous of Eastern Pontides, NE Turkey. Turkish Journal of Earth Sciences 20, 179–183.
Kandemir, R., Yılmaz, C., 2009. Lithostratigraphy, facies, and deposition environment of the lower Jurassic Ammonitico Rosso type sediments (ARTS) in the Gümüşhane area, NE Turkey: implications for the opening of the northern branch of the Neo-Tethys Ocean. Journal of Asian Earth Sciences 34, 586–598.
Kaygusuz, A., Arslan, M., Siebel, W., Sipahi, F., Ilbeyli, N., 2012. Geochronological evidence and tectonic significance of Carboniferous magmatism in the southwest Trabzon area, eastern Pontides, Turkey. International Geology Review 54, 1776–1800.

Please cite this article as: Dokuz, A., et al., Geochemistry, Re–Os isotopes and highly siderophile element abundances in the Eastern Pontide peridotites (NE Turkey): Multiple episodes ..., Gondwana Research (2014), http://dx.doi.org/10.1016/j.gr.2013.12.010

Kelemen, P.B., Shimizu, N., Salters, V.J.M., 1995. Extraction of mid-ocean-ridge basalt from the upwelling mantle by focused flow of melt in dunite channels. Nature 375, 747–753.

Kelemen, P.B., Hirth, G., Shimizu, N., Spiegelman, M., Dick, H.J.B., 1997. A review of melt migration processes in the adiabatically upwelling mantle beneath oceanic spreading ridges. Philos. Transactions Royal Society London 355, 283–318.

Kroner, U., Hahn, T., Romer, R.L., Linnemann, U., 2007. The Variscan orogeny in the Saxo-Thuringian Zone—heterogenous overprint of Cadomian/Palaeozoic Peri-Gondwana crust. In: Linnemann, U., Nance, R.D., Kraft, P., Zulauf, G. (Eds.), The Evolution Of The Rheic Ocean: From Avalonian–Cadomian Active Margin To Alleghenian–Variscan Collision. Geological Society of America Special Paper, 423, pp. 153–172.

Le Roux, V., Bodinier, J.-L., Tommasi, A., Alard, O., Dautria, J.-M., Vauchez, A., Riches, A.J.V., 2007. The Lherz spinel lherzolite: refertilized rather than pristine mantle. Earth and Planetary Science Letters 259, 599–612.

Levasseur, S., Birck, J.-L., Allègre, C.J., 1998. Direct measurement of femtomoles of osmium and the $^{187}Os/^{188}Os$ ratio in seawater. Science 282, 272–274.

Lorand, J.-P., Alard, O., 2001. Platinum-group element abundances in the upper mantle: new constraints from in-situ and whole rock analyses of massif Central xenoliths (France). Geochimica et Cosmochimica Acta 65, 2789–2806.

Lorand, J.-P., Gros, M., Pattou, L., 1999. Fractionation of platinum-group element in the upper mantle: a detailed study in Pyrenean orogenic peridotites. Journal of Petrology 40, 951–987.

Lorand, J.-P., Delpech, G., Gregoire, M., Moine, B., O'Reilly, S.Y., Cottin, J.Y., 2004. Platinum-group elements and the multistage metasomatic history of Kerguelen lithospheric mantle (South Indian Ocean). Chemical Geology 208, 195–215.

Lorand, J.-P., Luguet, A., Alard, O., Bezos, A., Meisel, T., 2008. Abundance and distribution of platinum-group elements in orogenic lherzolites; a case study in a Fontete Rouge lherzolite (French Pyrenees). Chemical Geology 248, 174–194.

Luguet, A., Lorand, J.-P., Alard, O., Cottin, J.Y., 2004. A multi-technique study of platinum group element systematic in some Ligurian ophiolitic peridotites, Italy. Chemical Geology 208, 175–194.

Luguet, A., Shirey, S.B., Lorand, J.-P., Horan, M.F., Carlson, R.W., 2007. Residual platinum-group minerals from highly depleted harzburgites of the Lherz massif (France) and their role in HSE fractionation of the mantle. Geochimica et Cosmochimica Acta 71, 3082–3097.

Mallmann, G., O'Neill, H.S.C., 2007. The effect of oxygen fugacity on the partitioning of Re between crystals and silicate melt during mantle melting. Geochimica et Cosmochimica Acta 71, 2837–2857.

Mavrogenes, J., O'Neill, H.S.C., 1999. The relative effects of pressure, temperature and oxygen fugacity on the solubility of sulfide in mafic magmas. Geochimica et Cosmochimica Acta 63, 1173–1180.

McDonough, W.F., Sun, S.S., 1995. The composition of the Earth. Chemical Geology 120, 223–253.

Meibom, A., Sleep, N.H., Chamberlain, C.P., Coleman, R.G., Frei, R., Hren, M.T., Wooden, J.L., 2002. Re–Os isotopic evidence for long-lived heterogeneity and equilibration processes in the Earth's upper mantle. Nature 419, 705–708.

Meisel, T., Moser, J., 2004. Reference materials for geochemical PGE analysis: new analytical data for Ru, Rh, Pd, Os, Ir, Pt and Re by isotope dilution ICP-MS in 11 geological reference materials. Chemical Geology 208, 319–338.

Meisel, T., Walker, R.J., Morgan, J.W., 1996. The osmium isotopic composition of the Earth's primitive upper mantle. Nature 383, 517–520.

Meisel, T., Walker, R.J., Irving, A.J., 2001. Osmium isotopic compositions of mantle xenoliths: a global perspective. Geochimica et Cosmochimica Acta 65, 1311–1323.

Meisel, T., Fellner, N., Moser, J., 2003. A simple procedure for the determination of platinum group elements and rhenium (Ru, Rh, Pd, Re, Os, Ir and Pt) using ID-ICP-MS with an inexpensive on-line matrix separation in geological and environmental materials. Journal of Analytical Atomic Spectrometry 18, 720–726.

Morgan, J.W., 1986. Ultramafic xenoliths: clues to Earth's late accretionary history. Journal of Geophysical Research 91, 12375–12387.

Morgan, J.W., Walker, R.J., Brandon, A.D., Horan, M.F., 2001. Siderophile elements in Earth's upper mantle and lunar breccias: data synthesis suggests manifestations of the same late influx. Meteorics and Planetary Science 36, 1257–1275.

Mungall, J.E., Andrews, D.R.A., Cabri, L.J., Sylvester, P.J., Tubrett, M., 2005. Partitioning of Cu, Ni, Au and platinum group elements between monosulfide solid solution and sulfide melt under controlled oxygen and sulfur fugacities. Geochimica et Cosmochimica Acta 69, 4349–4360.

Müntener, O., Pettke, T., Desmurs, L., Meier, M., Schaltegger, U., 2004. Re-fertilization of mantle peridotite in embryonic ocean basins: trace element and Nd isotopic evidence and implications for crust–mantle relationships. Earth and Planetary Science Letters 221, 293–308.

Murphy, J.B., Keppie, J.D., Nance, R.D., Dostal, J., 2010. Comparative evolution of the Iapetus and Rheic oceans: a North America perspective. Gondwana Research 17, 482–499.

Murphy, J.B., Cousens, B.L., Braid, J.A., Strachan, R.A., Dostal, J., Keppie, J.D., Nance, R.D., 2011. Highly depleted oceanic lithosphere in the Rheic ocean: implications for Paleozoic plate reconstructions. Lithos 123, 165–175.

Nance, R.D., Gutiérrez-Alonso, G., Keppie, J.D., Linnemann, U., Murphy, J.B., Quesada, C., Strachan, R.A., Woodcock, N., 2010. The evolution of the Rheic Ocean. Gondwana Research 17, 194–222.

O'Driscoll, B., Day, J.M.D., Walker, R.J., Daly, S.D., McDonough, W.F., Piccoli, P.M., 2012. Chemical heterogeneity in the upper mantle recorded by peridotites and chromitites from the Shetland Ophiolite Complex, Scotland. Earth and Planetary Science Letters 333–334, 226–237.

Okay, A., Leven, E.J., 1996. Stratigraphy and paleontology of the Upper Paleozoic sequences in the Pulur (Bayburt) region, Eastern Pontides. Turkish Journal of Earth Sciences 5, 145–155.

Okay, A.I., Satir, M., Siebel, W., 2006. Pre-Alpide Palaeozoic and Mesozoic orogenic events in the Eastern Mediterranean region. Geological Society of London Memoir 32, 389–405.

Ottley, C.J., Pearson, D.G., Irvine, G.J., 2003. A routine method for the dissolution of geological samples for the analysis of REE and trace elements via ICP-MS. In: Holland, J.G., Taner, S.D. (Eds.), Plasma Source Mass Spectrometry, Applications and Emerging Technologies. The Roy. Soc. Chem. Cambridge, U.K, pp. 221–230.

Paliulionyte, V., Meisel, T., Ramminger, P., Kettisch, P., 2006. High pressure asher digestions and ID-ICP-MS method for the determination of PGE concentrations in chromitite reference materials CHR-Bkg, GAN Pt-1and HHH. Geostandards and Geoanalytical Research 30, 87–96.

Paulick, H., Bach, W., Godard, M., De Hoog, J.C.M., Suhr, G., Harvey, J., 2006. Geochemistry of abyssal peridotites (Mid-Atlantic Ridge, 15°20′N, ODP Leg 209): implications for fluid/rock interaction in slow spreading environments. Chemical Geology 234, 19–210.

Pearson, D.G., Shirey, S.B., Carlson, R.W., Boyd, F.R., Pokhilenko, N.P., Shimizu, N., 1995. Re–Os, Sm–Nd and Rb–Sr isotope evidence for thick Archean lithospheric beneath the Siberian craton modified by multistage metasomatism. Geochimica et Cosmochimica Acta 59, 959–977.

Pearson, D.G., Canil, D., Shirey, S.B., 2003. Mantle samples included in volcanic rocks: xenoliths and diamonds. Treatise on Geochemistry, Part 2.Elsevier Ltd. 171–225.

Pearson, D.G., Irvine, G.J., Ionov, D.A., Boyd, F.R., Dreibus, G.E., 2004. Re–Os isotope systematics and platinum group element fractionation during mantle melt extraction: a study of massif and xenolith peridotite suites. Chemical Geology 208, 29–59.

Piccardo, G.B., 2003. Mantle processes during ocean formation: petrologic records in peridotites from the Alpine–Apennine ophiolites. Episodes 26, 193–199.

Potts, P.J., Tindle, A.G., Webb, P.C., 1992. Geochemical Reference Materials Compositions: Rocks, Minerals, Sediments, Soils, Carbonates, Refractories and Ores Used in Research and Industry. Whittles Publishing, Caithness, U.K.

Rajabzadeh, M.A., Dehkordi, T.N., Caran, Ş., 2013. Mineralogy, geochemistry and geotectonic significance of mantle peridotites with high-Cr chromitites in the Neyriz ophiolite from the outer Zagros ophiolite belts, Iran. Journal of African Earth Sciences 78, 1–15.

Rampone, E., Borghini, G., 2008. Melt migration and intrusion in the Erro–Tobbio peridotites (Ligurian Alps, Italy): insights on lithospheric processes in extending lithospheric mantle. European Journal of Mineralogy 20, 573–585.

Rampone, E., Romairone, A., Hofmann, A.W., 2004. Contrasting bulk and mineral chemistry in depleted mantle peridotites: evidence for reactive porous flow. Earth and Planetary Science Letters 218, 491–506.

Rampone, E., Piccardo, G., Hofmann, A., 2008. Multi-stage melt–rock interaction in the Mt. Maggiore (Corsica, France) ophiolitic peridotites: microstructural and geochemical evidence. Contributions to Mineralogy and Petrology 156, 453–475.

Rehkämper, M., Halliday, A.N., Alt, J., Fitton, J.G., Zipfel, J., Takazawa, E., 1999a. Non-chondritic platinum-group element ratios in oceanic mantle lithosphere: petrogenetic signature of melt percolation? Earth and Planetary Science Letters 172, 65–81.

Rehkämper, M., Halliday, A.N., Fitton, J.G., Lee, D.C., Wieneke, M., Arndt, N.T., 1999b. Ir, Ru, Pt, and Pd in basalts and komatiites: new constraints for the geochemical behavior of the platinum-group elements in the mantle. Geochimica et Cosmochimica Acta 63, 3915–3934.

Reisberg, L., Lorand, J.-P., 1995. Longevity of sub-continental mantle lithosphere from osmium isotope systematics in orogenic peridotite massifs. Nature 376, 159–162.

Reisberg, L., Zhi, X., Lorand, J.-P., Wagner, C., Peng, Z., Zimmermann, C., 2005. Re–Os and S systematics of spinel peridotite xenoliths from east central China: evidence for contrasting effects of melt percolation. Earth and Planetary Science Letters 239, 286–308.

Righter, K., Hauri, E.H., 1998. Compatibility of rhenium in garnet during mantle melting and magma genesis. Science 280, 1737–1741.

Righter, K., Campbell, A.J., Humayun, M., Hervig, R.L., 2004. Partitioning of Ru, Rh, Pd, Re, Ir and Au between Cr-bearing spinel, olivine, pyroxene and silicate melts. Geochimica et Cosmochimica Acta 68, 867–880.

Roy-Barman, M., Wasserburg, G.J., Papanastassiou, D.A., Chaussidon, M., 1998. Osmium isotopic compositions and Re–Os concentrations in sulfide globules from basaltic glasses. Earth and Planetary Science Letters 154, 331–347.

Saal, A.E., Takazawa, E., Frey, F.A., Shimizu, N., Hart, S.R., 2001. Re–Os isotopes in the Horoman peridotite: evidence for re-fertilization? Journal of Petrology 42, 25-24.

Sarifakioglu, E., Dilek, Y., Sevin, M., 2013. Jurassic–Paleogene intra-oceanic magmatic evolution of the Ankara Mélange, North-Central Anatolia, Turkey. Solid Earth 5. http://dx.doi.org/10.5194/sed-5-1-2013.

Sattari, P., Brenan, J.M., Horn, I., McDonough, W.F., 2002. Experimental constraints on the sulfide- and chromite-silicate melt partitioning behavior of rhenium and platinum-group elements. Economic Geology 97, 385–398.

Schiano, P., Birck, J.-L., Allègre, C.J., 1997. Osmium–strontium–neodymium–lead isotopic covariations in mid-ocean ridge basalt glasses and the heterogeneity of the upper mantle. Earth and Planetary Science Letters 150, 363–379.

Schmidt, G., Snow, J.E., 2002. Os isotopes in mantle xenoliths from the Eifel volcanic field and the Vogelsberg (Germany): age constraints on the lithospheric mantle. Contributions to Mineralogy and Petrology 143, 694–705.

Şen, C., 2007. Jurassic volcanism in the Eastern Pontides: is it rift related or subduction related? Turkish Journal of Earth Sciences 16, 523–539.

Seyler, M., Lorand, J.-P., H.B.J., Drouin, M., 2007. Pervasive melt–percolation reactions in ultra-depleted refractory harzburgites at the Mid-Atlantic Ridge, 15–20 N, ODP Hole 1274. Contributions to Mineralogy and Petrology 153, 303–319.

Shi, R., Alard, O., Zhi, X.-C., O'Reilly, S.Y., Pearson, N.J., Griffin, W.L., Zhang, M., Chen, X.-M., 2007. Multiple events in the Neo-Tethyan oceanic upper mantle: evidence from Ru–Os–Ir alloys in the Luobusa and Dongqiao ophiolitic podiform chromitites, Tibet. Earth and Planetary Science Letters 261, 33–48.

Please cite this article as: Dokuz, A., et al., Geochemistry, Re–Os isotopes and highly siderophile element abundances in the Eastern Pontide peridotites (NE Turkey): Multiple episodes ..., Gondwana Research (2014), http://dx.doi.org/10.1016/j.gr.2013.12.010

Shi, R., Griffin, W.L., O'Reilly, S.Y., Huang, Q., Zhang, X., Liu, D., Zhi, X., Xia, Q., Ding, L., 2012. Melt/mantle mixing produces podiform chromite deposits in ophiolites: implications of Re–Os systematics in the Dongqiao Neo-tethyan ophiolite, northern Tibet. Gondwana Research 21, 194–206.
Shirey, S.B., Walker, R.J., 1998. The Re–Os isotope system in cosmochemistry and high-temperature geochemistry. Annual Review of Earth and Planetary Sciences 26, 423–500.
Snow, J.E., Dick, H.J.B., 1995. Pervasive magnesium loss by marine weathering of peridotite. Geochimica et Cosmochimica Acta 59, 4219–4235.
Snow, J.E., Reisberg, L., 1995. Os isotopic systematics of the MORB mantle: results from altered abyssal peridotites. Earth and Planetary Science Letters 136, 723–733.
Standish, J.J., Hart, S.R., Blusztajn, J., Dick, H.J.B., Lee, K.L., 2002. Abyssal peridotite osmium isotopic compositions from Cr-spinel. Geochemistry Geophysics Geosystems. AGU and the Geochemical Society. http://dx.doi.org/10.1029/2001GC000161.
Staudigel, H., Plank, T., White, B., Schmincke, H.-U., 1996. Geochemical fluxes during seafloor alteration of the basaltic upper oceanic crust: DSDP sites 417 and 418. In: Bebout, G. (Ed.), Subduction: Top to Bottom. American Geophysical Union, vol. 96, pp. 19–38.
Stracke, A., Bourdon, B., 2009. The importance of melt extraction for tracing mantle heterogeneity. Geochimica et Cosmochimica Acta 73, 218–238.
Sun, W., Bennett, V.C., Eggins, S.M., Arculus, R.J., Perfit, M.R., 2003. Rhenium systematics in submarine MORB and back-arc basin glasses: laser ablation ICP-MS results. Chemical Geology 196, 259–281.
Takazawa, E., Frey, F.A., Shimuzu, N., Obata, M., 2000. Whole rock compositional variations in an upper mantle peridotite (Horoman, Hokkaido, Japan): are they consistent with a partial melting process? Geochimica et Cosmochimica Acta 64, 695–716.
Topuz, G., Altherr, R., Satır, M., Schwarz, W.H., 2004. Low-grade metamorphic rocks from the Pulur complex, NE Turkey: implications for the pre-Liassic evolution of the Eastern Pontides. International Journal of Earth Sciences 93, 72–91.
Topuz, G., Altherr, R., Schwarz, W.H., Dokuz, A., Meyer, H.P., 2007. Variscan amphibolite-facies rocks from the Kurtoğlu metamorphic complex, Gümüşhane area, Eastern Pontides, Turkey. International Journal of Earth Sciences 96, 861–873.
Toramaru, T., Takazawa, E., Morishita, T., Matsukage, K., 2001. Model of layering formation in a mantle peridotite (Horoman, Hokkaido, Japan). Earth and Planetary Science Letters 185, 299–313.
Ustaömer, T., Robertson, A.H.F., 2010. Late Palaeozoic–Early Cenozoic tectonic development of the Eastern Pontides (Artvin area), Turkey: stages of closure of Tethys along the southern margin of Eurasia. Geological Society, London, Special Publications 340, 281–327.
Uysal, I., Ersoy, E.Y., Karslı, O., Dilek, Y., Sadiklar, M.B., Ottley, C.J., Tiepolo, M., Meisel, T., 2012. Coexistence of abyssal and ultra-depleted SSZ type mantle peridotites in a Neo-Tethyan Ophiolite in SW Turkey: constraints from mineral composition, whole-rock geochemistry (major–trace–REE–PGE), and Re–Os isotope systematics. Lithos 132–133, 50–69.
van Acken, D., Becker, H., Walker, R.J., 2008. Re-fertilization of Jurassic oceanic peridotites from the Tethys ocean: implications for the Re–Os systematics of the upper mantle. Earth and Planetary Science Letters 268, 171–181.
van Acken, D., Becker, H., Hammerschmidt, K., Walker, R.J., Wombacher, F., 2010. Highly siderophile elements and Sr–Nd isotopes in refertilized mantle peridotites — a case study from the Totalp ultramafic body, Swiss Alps. Chemical Geology 276, 257–268.
Varfalvy, V., Hebert, R., Bedard, J.H., 1996. Interactions between melt and upper-mantle peridotites in the North Arm Mountain massif, Bay of Islands ophiolite, Newfoundland, Canada: Implications for the genesis of boninitic and related magmas. Chemical Geology 129, 71–90.
Walker, R.J., 2009. Highly siderophile elements in the Earth, Moon and Mars: update and implications for planetary accretion and differentiation. Chemie der Erde 69, 101–125.
Walker, R.J., Carlson, R.W., Shirey, S.B., Boyd, F.R., 1989. Os, Sr, Nd, and Pb isotope systematics of southern African peridotite xenoliths: implications for the chemical evolution of the subcontinental mantle. Geochimica et Cosmochimica Acta 53, 1583–1595.
Walker, R.J., Prichard, H.M., Ishiwatari, A., Pimentel, M., 2002. The osmium isotopic composition of convecting upper mantle deduced from ophiolite chromites. Geochimica et Cosmochimica Acta 66, 329–345.
Walter, M.J., 2003. Melt extraction and compositional variability in mantle lithosphere. In: Holland, H.D., Turekian, K.K. (Eds.), Treatise on Geochemistry. Elsevier, Amsterdam, pp. 363–394.
Wendt, I., Carl, C., 1991. The statistical distribution of the mean squared weighted deviation. Chemical Geology 86, 275–285.
Wong, K., Sun, M., Zhao, G., Yuan, C., Xiao, W.-J., 2010. Geochemical and geochronological studies of the Alegedayi Ophiolitic Complex and its implication for the evolution of the Chinese Altai. Gondwana Research 18, 438–454.
Wood, 1987. Thermodynamic calculations of the volatility of the platinum group elements (PGE): the PGE content of fluids at magmatic temperatures. Geochimica et Cosmochimica Acta 51, 3041–3050.
Xu, X.-Z., Yang, J., Ba, D.-Z., Guo, G., Robinson, P.T., Li, J.-Y., 2011. Petrogenesis of the Kangjinla peridotite in the Luobusa ophiolite, Southern Tibet. Journal of Asian Earth Sciences 42, 553–568.
Yilmaz, Y., Tüysüz, O., Yigitbas, E., Genc, S.C., Sengor, A.M.C., 1997. Geology and tectonic evolution of the Pontides. In: Robinson, A.G. (Ed.), Regional and Petroleum Geology of the Black Sea and Surrounding Region. AAPG Memoir, 68, pp. 183–226.
Yoshikawa, M., Ozawa, K., 2007. Rb–Sr and Sm–Nd isotopic systematics of the Hayachine–Miyamori ophiolitic complex: melt generation process in the mantle wedge beneath an Ordovician island arc. Gondwana Research 11, 234–246.
Zhou, M.-F., Robinson, P.T., Malpas, J., Li, Z., 1996. Podiform chromitites in the Luobusa ophiolite (Southern Tibet): implications for melt–rock interaction and chromite segregation in the upper mantle. Journal of Petrology 37, 3–21.

Please cite this article as: Dokuz, A., et al., Geochemistry, Re–Os isotopes and highly siderophile element abundances in the Eastern Pontide peridotites (NE Turkey): Multiple episodes ..., Gondwana Research (2014), http://dx.doi.org/10.1016/j.gr.2013.12.010